Downloaded from orbit.dtu.dk on: May 05, 2023

DTU Library

Surface Display of Small Affinity Proteins on Synechocystis sp Strain PCC 6803 Mediated by Fusion to the Major Type IV Pilin PilA1

Cengic, Ivana; Uhlén, Mathias; Hudson, Elton P.

Published in:
Journal of Bacteriology

Link to article, DOI:
10.1128/JB.00270-18

Publication date:
2018

Document Version
Publisher's PDF, also known as Version of record

Link back to DTU Orbit

Citation (APA):
Cengic, I., Uhlén, M., & Hudson, E. P. (2018). Surface Display of Small Affinity Proteins on *Synechocystis* sp Strain PCC 6803 Mediated by Fusion to the Major Type IV Pilin PilA1. *Journal of Bacteriology*, *200*(16), [e00270-18]. https://doi.org/10.1128/JB.00270-18

General rights
Copyright and moral rights for the publications made accessible in the public portal are retained by the authors and/or other copyright owners and it is a condition of accessing publications that users recognise and abide by the legal requirements associated with these rights.

- Users may download and print one copy of any publication from the public portal for the purpose of private study or research.
- You may not further distribute the material or use it for any profit-making activity or commercial gain
- You may freely distribute the URL identifying the publication in the public portal

If you believe that this document breaches copyright please contact us providing details, and we will remove access to the work immediately and investigate your claim.

AMERICAN SOCIETY FOR MICROBIOLOGY | Journal of Bacteriology®

RESEARCH ARTICLE

Surface Display of Small Affinity Proteins on *Synechocystis* sp. Strain PCC 6803 Mediated by Fusion to the Major Type IV Pilin PilA1

Ivana Cengic,[a] Mathias Uhlén,[a,b] Elton P. Hudson[a]

[a]School of Engineering Sciences in Chemistry, Biotechnology, and Health, KTH Royal Institute of Technology, Science for Life Laboratory, Stockholm, Sweden

[b]Novo Nordisk Foundation Center for Biosustainability, Technical University of Denmark, Hørsholm, Denmark

ABSTRACT Functional surface display of small affinity proteins, namely, affibodies (6.5 kDa), was evaluated for the model cyanobacterium *Synechocystis* sp. strain PCC 6803 through anchoring to native surface structures. These structures included confirmed or putative subunits of the type IV pili, the S-layer protein, and the heterologous *Escherichia coli* autotransporter antigen 43 system. The most stable display system was determined to be through C-terminal fusion to PilA1, the major type IV pilus subunit in *Synechocystis*, in a strain unable to retract these pili (Δ*pilT1*). Type IV pilus synthesis was upheld, albeit reduced, when fusion proteins were incorporated. However, pilus-mediated functions, such as motility and transformational competency, were negatively affected. Display of affibodies on *Synechocystis* and the complementary anti-idiotypic affibodies on *E. coli* or *Staphylococcus carnosus* was able to mediate interspecies cell-cell binding by affibody complex formation. The same strategy, however, was not able to drive cell-cell binding and aggregation of *Synechocystis*-only mixtures. Successful affibody tagging of the putative minor pilin PilA4 showed that it locates to the type IV pili in *Synechocystis* and that its extracellular availability depends on PilA1. In addition, affibody tagging of the S-layer protein indicated that the domains responsible for the anchoring and secretion of this protein are located at the N and C termini, respectively. This study can serve as a basis for future surface display of proteins on *Synechocystis* for biotechnological applications.

IMPORTANCE Cyanobacteria are gaining interest for their potential as autotrophic cell factories. Development of efficient surface display strategies could improve their suitability for large-scale applications by providing options for designed microbial consortia, cell immobilization, and biomass harvesting. Here, surface display of small affinity proteins was realized by fusing them to the major subunit of the native type IV pili in *Synechocystis* sp. strain PCC 6803. The display of complementary affinity proteins allowed specific cell-cell binding between *Synechocystis* and *Escherichia coli* or *Staphylococcus carnosus*. Additionally, successful tagging of the putative pilin PilA4 helped determine its localization to the type IV pili. Analogous tagging of the S-layer protein shed light on the regions involved in its secretion and surface anchoring.

KEYWORDS surface display, cyanobacteria, affibody, type IV pili, S-layer protein, cell-cell binding

Cyanobacteria are emerging as attractive alternative microbial production hosts for the photosynthesis-driven conversion of CO_2 to biofuels and platform chemicals (1–3). *Synechocystis* sp. strain PCC 6803 has emerged as a model organism; however, many biotechnological tools available for other commonly engineered microbes, such

Received 2 May 2018 **Accepted** 22 May 2018

Accepted manuscript posted online 29 May 2018

Citation Cengic I, Uhlén M, Hudson EP. 2018. Surface display of small affinity proteins on *Synechocystis* sp. strain PCC 6803 mediated by fusion to the major type IV pilin PilA1. J Bacteriol 200:e00270-18. https://doi.org/10.1128/JB.00270-18.

Editor Conrad W. Mullineaux, Queen Mary University of London

Copyright © 2018 American Society for Microbiology. All Rights Reserved.

Address correspondence to Elton P. Hudson, huds@kth.se.

Downloaded from http://jb.asm.org/ on August 9, 2018 by TECH KNOWLEDGE CTR OF DENMARK

as *Escherichia coli* and *Saccharomyces cerevisiae*, are still underdeveloped for cyanobacteria. One such tool is a surface display platform, where the diverse range of applications (4) can be useful for optimizing aspects of microbial production hosts. For example, surface display of polymerizing proteins on different organisms could aid in constructing synthetic microbial communities and engineered biofilm structures. The development of synthetic consortia has gained interest due to its potential for creating more complex and robust systems, which could aid in, e.g., biofuel production applications (5). Here, cyanobacteria could produce the sugars required by engineered heterotrophs (6–8). Display of polymerizing proteins could also be used for controlled flocculation by self-aggregation and thus facilitate harvesting of biomass without the need for externally added flocculants (9, 10). This could help avoid chemical contamination of the biomass and growth media while also reducing harvesting costs.

Multiple aspects of cyanobacteria challenge the realization of useful surface display systems. These Gram-negative bacteria have an unusually thick and highly cross-linked peptidoglycan layer (11). In addition, the intracellular thylakoid membranes could become targets for incorrect anchor insertion (12). Many species also synthesize and assemble protective extracellular S-layers (13) and secrete polysaccharide substances that form cell-enveloping capsules, sheaths, or slimes (14). Native proteins could be advantageous as carriers for functional display since they are already capable of successfully navigating the complex cell wall structure of cyanobacteria. Surface structures commonly used as carriers in other bacteria include subunits of polymeric surface appendages such as pili or flagella, S-layer proteins, or outer membrane proteins (4).

Some success in surface display on cyanobacteria has been reported. Organophosphorus hydrolase from *Flavobacterium* sp. was displayed on *Synechococcus elongatus* PCC 7942 using the truncated ice nucleation protein from *Pseudomonas syringae* (15) as well as through a truncating insertion into a proposed extracellular loop of the native porin SomA (16). However, in both cases, the hydrolase was only partially accessible to proteases targeting extracellular structures, suggesting incomplete display. Recently, the successful display of a FLAG epitope on *S. elongatus* was realized by sandwich insertion into a predicted extracellular loop of SomA (17). The extracellular display of the FLAG epitope and the external addition of an anti-FLAG antibody were able to mediate adherence between *S. elongatus* and protein A-expressing yeast or protein A-coupled beads (17). In *Synechocystis*, a surface display method utilizing *E. coli* antigen 43, an autotransporter protein, was able to display the native antigen 43 passenger domain (18).

In this work, several native surface structures on *Synechocystis* sp. PCC 6803 were explored as possible carrier proteins to mediate the surface display of a 6.5-kDa affibody (19). Affibodies are small (6.5-kDa) engineered affinity proteins with exceptional stability and rapid folding (19). They are based on the immunoglobulin-binding B domain of staphylococcal protein A (20). In this work, the carriers evaluated for allowing surface display included the S-layer protein (21), the major type IV pilus subunit PilA1 (22), and the two putative pilin proteins PilA2 and PilA4 (23). In addition, display using the heterologous *E. coli* antigen 43 autotransporter was also evaluated. Our established display system was further tested for its ability to mediate inter- and intraspecies cell-cell binding due to the display of complementary complex-forming affibodies.

RESULTS

Selection of surface structures to evaluate as carrier proteins. *Synechocystis* cells are covered in protruding appendages of both thick and thin morphologies (22). The thick appendages have been classified as type IV pili and are important for motility and natural transformation competency (22, 23). Successful fusion to the protein subunits of the pilus could provide a high level of surface display due to its polymeric nature. The major pilin protein, which makes up the majority of the type IV pilus structure, has been identified in *Synechocystis* as PilA1 (*sll1694* product) (22). There are nine additional

Downloaded from http://jb.asm.org/ on August 9, 2018 by TECH KNOWLEDGE CTR OF DENMARK

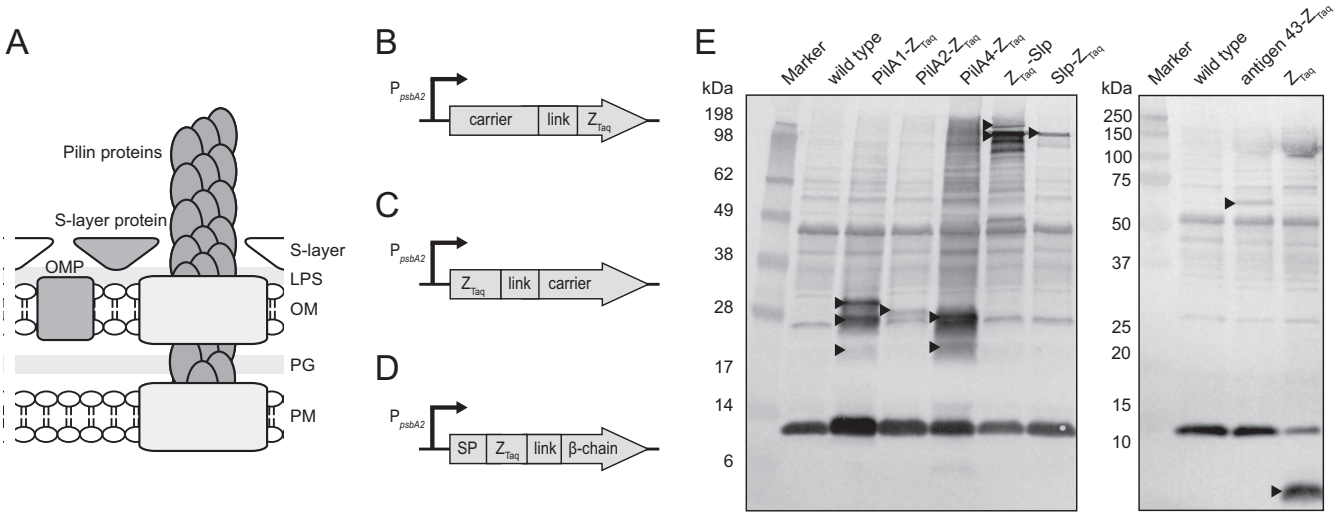

FIG 1 (A) Simplified schematic of the cell wall architecture of *Synechocystis*. Proteins evaluated as carriers for surface display are marked in dark gray, including the S-layer protein, three pilin proteins (PilA1, PilA2, and PilA4), and the heterologous *E. coli* antigen 43, which would be embedded in the outer membrane. Abbreviations: LPS, lipopolysaccharide layer; OM, outer membrane; PG, peptidoglycan; PM, plasma membrane; OMP, outer membrane protein. (B to D) Schematics showing the construction of the fusion proteins for a C-terminal fusion to the evaluated pilin and S-layer protein carriers (B), an N-terminal fusion to the evaluated S-layer protein carrier (C), and an insertion of the Z_{Taq} affibody instead of the native passenger domain for the antigen 43 autotransporter (D). The signal peptide (SP) and β-chain translocation domain were kept as they are. (E) Immunoblot against Z_{Taq} of whole-cell extracts of *Synechocystis* strains expressing the fusion proteins. From left to right (including both blots) are a marker, the wild-type negative control, PilA1-Z_{Taq}, PilA2-Z_{Taq}, PilA4-Z_{Taq}, Z_{Taq}-Slp, Slp-Z_{Taq}, a marker, the wild-type negative control, antigen 43-Z_{Taq}, and a Z_{Taq} intracellular control. Arrowheads indicate the bands belonging to the fusion proteins.

genes in the *Synechocystis* genome displaying prepilin gene characteristics (24). The putative pilin PilA2 (*sll1695* product) is transcribed from the same operon as PilA1, and together, they are the *Synechocystis* pilins showing the highest similarity to the major pilin protein in the highly characterized pilus structures of *Pseudomonas aeruginosa* and *Myxococcus xanthus* (25). Upregulated transcription of both *pilA1* and *pilA4* (*slr1456*) has been observed upon exposure to external stresses such as butanol (26), benzyl alcohol (27), and carbon limitation (28), indicating potentially concerted expression. These three pilin proteins (PilA1, PilA2, and PilA4) were chosen as potential carrier proteins for evaluation of the surface display of affibodies.

The S-layer protein (*sll1951* product) of *Synechocystis* is the only component of its paracrystalline S-layer, which makes up the outermost cell surface (21). Successful fusion to the S-layer protein could provide a cell completely covered in fusion proteins, and it was therefore included in the set of carrier proteins for evaluation.

Outer membrane proteins are common carriers that allow the covalent anchoring of displayed proteins on the cell surface (4). The *E. coli* antigen 43 autotransporter system has previously been successfully expressed in *Synechocystis*, where it was able to mediate the display of its native passenger domain (18). Here, the antigen 43 system was thus evaluated for its ability to instead mediate the display of an affibody as the passenger.

A schematic showing the cell wall architecture of *Synechocystis* as well as the location of the proteins evaluated as carriers for surface display is shown in Fig. 1A.

Construction and confirmed expression of carrier-passenger fusion proteins. The affibody $Z_{Taq\ S1\text{-}1}$ (here Z_{Taq}) (29) was used as the passenger protein in this study. Fusions between the selected carriers and the Z_{Taq} passenger were done by either N- or C-terminal fusion, depending on the characteristics of the carrier (Fig. 1B to D and Table 1). A flexible linker region (GSSSGSS) was included between the fused proteins to avoid potential structural disruption. All constructed fusion proteins were expressed under the control of the moderate P_{psbA2} promoter (30), from a replicative plasmid. A nonmotile *Synechocystis* strain was used as the main host in this study.

For all evaluated pilins (PilA1, PilA2, and PilA4), the Z_{Taq} fusion occurred at their C termini (Fig. 1B), as prepilins have N-terminal signal peptides that are cleaved off

Downloaded from http://jb.asm.org/ on August 9, 2018 by TECH KNOWLEDGE CTR OF DENMARK

TABLE 1 Strains and plasmids used in this study

Strain or plasmid	Relevant characteristic(s) or genotype	Source and/or reference
Strains		
Escherichia coli		
XL1-Blue	Cloning host	Stratagene
BL21(DE3)	Host for AIDA-I constructs	Novagen
Z_{Taq} strain	pAraBADmin-Z_{Taq}; BL21(DE3)	This study
AntiZ_{Taq} strain	pAraBADmin-antiZ_{Taq}; BL21(DE3)	This study
Staphylococcus carnosus		
Z_{Taq} strain	pSCEM2-Z_{Taq} (Cm^r)	J. Löfblom
AntiZ_{Taq} strain	pSCEM2-antiZ_{Taq} (Cm^r)	J. Löfblom
Z_{IgG} strain	pSCEM2-Z_{IgG} (Cm^r)	J. Löfblom
Synechocystis sp. PCC 6803		
Wild type (nonmotile)	Nonmotile; GT-S derivative; main host in this study	M. Fulda
Wild type (motile)	Motile	X. Lu
PilA1-Z_{Taq}	pJA2-PilA1-Z_{Taq}	This study
PilA1-Z_{Taq} (in motile host)	pJA2-PilA1-Z_{Taq}	This study
PilA2-Z_{Taq}	pJA2-PilA2-Z_{Taq}	This study
PilA4-Z_{Taq}	pJA2-PilA4-Z_{Taq}	This study
PilA4-Z_{Taq} (in motile host)	pJA2-PilA4-Z_{Taq}	This study
Z_{Taq}-Slp	pJA2-Z_{Taq}-Slp	This study
Slp-Z_{Taq}	pJA2-Slp-Z_{Taq}	This study
Antigen 43-Z_{Taq}	pJA2c-antigen 43-Z_{Taq}	This study
Z_{Taq}	pJA2-Z_{Taq}	This study
Z_{Taq} (in motile host)	pJA2-Z_{Taq}	This study
PilA1-antiZ_{Taq}	pJA2-PilA1-antiZ_{Taq}	This study
PilA1-antiZ_{Taq} Δ*pilT1*	pJA2-PilA1-antiZ_{Taq}; Δ*pilT1*::Sp^r	This study
Δ*pilA1*	Sp^r inserted to disrupt *pilA1* (*sll1694*)	This study
Δ*pilA4*	Cm^r inserted to disrupt *pilA4* (*slr1456*)	This study
Δ*pilT1*	Sp^r inserted to disrupt *pilT1* (*slr0161*)	This study
Δ*slp*	Sp^r inserted to disrupt *slp* (*sll1951*)	This study
PilA1-Z_{Taq} Δ*pilA1*	pJA2-PilA1-Z_{Taq}; Δ*pilA1*::Sp^r	This study
PilA1-Z_{Taq} Δ*pilT1*	pJA2-PilA1-Z_{Taq}; Δ*pilT1*::Sp^r	This study
PilA4-Z_{Taq} Δ*pilA4*	pJA2-PilA4-Z_{Taq}; Δ*pilA4*::Cm^r	This study
PilA4-Z_{Taq} Δ*pilT1*	pJA2-PilA4-Z_{Taq}; Δ*pilT1*::Sp^r	This study
PilA4-Z_{Taq} Δ*pilA1*	pJA2-PilA4-Z_{Taq}; Δ*pilA1*::Sp^r	This study
Z_{Taq} Δ*pilA1*	pJA2-Z_{Taq}; Δ*pilA1*::Sp^r	This study
Z_{Taq} Δ*pilT1*	pJA2-Z_{Taq}; Δ*pilT1*::Sp^r	This study
Z_{Taq} Δ*pilA4*	pJA2-Z_{Taq}; Δ*pilA4*::Cm^r	This study
Plasmids		
pJA2	Replicative plasmid; P_{psbA2} promoter; Km^r	26
pJA2c	Replicative plasmid; P_{psbA2} promoter; Cm^r	26
pType-IIs	Vector for Golden Gate assembly; Amp^r	Invitrogen
pAraBADmin-Z-EC	Replicative plasmid; arabinose-inducible gene expression; Cm^r	K. Andersson (54)
pJA2-PilA1-Z_{Taq}	Z_{Taq} C-terminally fused to *pilA1* (*sll1694*); Km^r	This study
pJA2-PilA2-Z_{Taq}	Z_{Taq} C-terminally fused to *pilA2* (*sll1695*); Km^r	This study
pJA2-PilA4-Z_{Taq}	Z_{Taq} C-terminally fused to *pilA4* (*sll1456*); Km^r	This study
pJA2-Z_{Taq}-Slp	Z_{Taq} N-terminally fused to S-layer protein (*sll1951*); Km^r	This study
pJA2-Slp-Z_{Taq}	Z_{Taq} C-terminally fused to S-layer protein (*sll1951*); Km^r	This study
pJA2c-antigen 43-Z_{Taq}	Z_{Taq} inserted in place of the native *E. coli* antigen 43 passenger domain; Cm^r	This study
pJA2-Z_{Taq}	Z_{Taq} expressed by itself; Km^r	This study
pJA2-PilA1-antiZ_{Taq}	AntiZ_{Taq} C-terminally fused to *pilA1* (*sll1694*); Km^r	This study
pAraBADmin-Z_{Taq}	Z_{Taq} inserted as a passenger for the AIDA-I display system; Cm^r	This study
pAraBADmin-antiZ_{Taq}	antiZ_{Taq} inserted as a passenger for the AIDA-I display system; Cm^r	This study
pType-IIs-Δ*slp*::Sp^r	Suicide vector for *slp* (*sll1951*) knockout; Amp^r Sp^r	This study
pType-IIs-Δ*pilA1*::Sp^r	Suicide vector for *pilA1* (*sll1694*) knockout; Amp^r Sp^r	This study
pType-IIs-Δ*pilA4*::Cm^r	Suicide vector for *pilA4* (*sll1456*) knockout; Amp^r Cm^r	This study
pType-IIs-Δ*pilT1*::Sp^r	Suicide vector for *pilT1* (*slr0161*) knockout; Amp^r Sp^r	This study
pMD19-Δ*psbA1*::Sp^r	Suicide vector for *psbA1* (*slr1181*) knockout; Amp^r Sp^r	L. Yao

by PilD during their maturation into pilins (24). In addition, the N-terminal part of the mature pilin forms a hydrophobic helix that is embedded in the middle of the helical pilus rod (31), making fusion to the N terminus unsuitable for display purposes.

Downloaded from http://jb.asm.org/ on August 9, 2018 by TECH KNOWLEDGE CTR OF DENMARK

Secretion of the S-layer protein (here Slp) in *Synechocystis* has been shown to be dependent on the TolC homolog Slr1270 (32) and, recently, two more accessory proteins of the type I secretion system (33). In addition, Slp is a member of the RTX (repeat-in-toxin) protein family, which is known to be secreted by the type I secretion system that utilizes noncleavable C-terminal signal peptides (34). However, the actual signal peptide for Slp in *Synechocystis* has not yet been described. Therefore, evaluating Slp as a carrier for surface display included fusing Z_{Taq} to either the C or N terminus (Fig. 1B and C). During the construction of the Slp fusion proteins, a frameshift resulting from a 76-bp deletion (bp 3127 to 3202) was discovered in the *sll1951* gene of the wild-type *Synechocystis* host used. Microevolution within the gene for Slp (*sll1951*) was observed previously in resequencing efforts for various laboratory *Synechocystis* strains (35, 36). The correct full-length gene, as specified by Cyanobase (37), was therefore amplified from another available wild-type strain.

For the heterologous *E. coli* antigen 43 system, the native passenger domain (amino acids 53 to 551) was exchanged for Z_{Taq} (Fig. 1D). The β-chain translocator domain was kept intact, as was the antigen 43 signal peptide, which was shown to mediate correct translocation in *Synechocystis* previously (18).

Functional expression of the correct Z_{Taq}-carrier fusion proteins in *Synechocystis* was evaluated by immunoblotting against the Z_{Taq} affibody (Fig. 1E). A strain expressing Z_{Taq} intracellularly was included as a positive control. The blots show a high degree of unspecific binding; however, comparison to the wild-type controls allowed the identification of the Z_{Taq} fusion proteins. All pilin-based fusion proteins showed bands of a larger-than-expected size (22.3 kDa for PilA1-Z_{Taq}, 22.9 kDa for PilA2-Z_{Taq}, and 23.6 kDa for PilA4-Z_{Taq}), even when accounting for predicted signal peptides (see Materials and Methods). PilA1 in *Synechocystis* undergoes several posttranslational modifications that are important for pilus assembly and function (38–40). It is possible that similar modifications also occur on PilA2 and PilA4, thus yielding larger-than-expected sizes for the fusion proteins. The multiple bands seen for PilA1-Z_{Taq} and PilA4-Z_{Taq} can also be explained by an incomplete modification of some of the protein pool. Both N- and C-terminal versions of the Slp-based Z_{Taq} fusion proteins were detected, whereby two bands were observed for the Z_{Taq}-Slp strain (Fig. 1E). This indicates that the Z_{Taq}-Slp but not the Slp-Z_{Taq}, fusion protein was able to undergo the glycosylation that is found on native Slp (21). Some degradation products could also be seen for the PilA1-Z_{Taq}, PilA4-Z_{Taq}, and Z_{Taq}-Slp strains. The heterologous antigen 43-Z_{Taq} strain yielded a band at the expected size (58.7 kDa), indicating the correct assembly of the fusion protein (Fig. 1E).

Assessing surface display of Z_{Taq} on *Synechocystis* by flow cytometry and immunofluorescence. The *Synechocystis* strains expressing Z_{Taq} fusion proteins were analyzed by flow cytometry to measure the surface availability of Z_{Taq} to an antiaffibody antibody. For a representative image of the gating procedure used to select the cyanobacterial population, see Fig. S1A in the supplemental material. The measured median fluorescence intensity (MFI) for all strains was normalized to the value obtained for a wild-type control, yielding relative MFI values. Analysis by immunofluorescence was also included in order to provide a visual comparison between strains and gauge the location of the Z_{Taq} affibody on the cells. More representative micrographs, in addition to the ones shown in Fig. 2, are shown in Fig. S2 in the supplemental material.

The construct using antigen 43 as a carrier did not mediate surface availability of the affibody but yielded only roughly background fluorescence levels (Fig. 2A and B). In contrast, fusion to PilA1 or PilA4 yielded a $>$2-fold increase in the relative MFI signal (Fig. 2A) and comparable labeling in the immunofluorescence assay (Fig. 2B). The use of PilA2 as a carrier also resulted in labeled cells when viewed with a microscope but at a smaller amount than for either PilA1-Z_{Taq} or PilA4-Z_{Taq}. The measured relative MFI for PilA2-Z_{Taq} reflected this lower display level by resulting in close-to-background fluorescence levels (Fig. 2A). For Slp, the fusion of Z_{Taq} to its N terminus (Z_{Taq}-Slp) gave a 10-fold increase and the highest relative MFI signal of all evaluated strains, while fusion to the C terminus (Slp-Z_{Taq}) showed a much lower level of functional display. In

Downloaded from http://jb.asm.org/ on August 9, 2018 by TECH KNOWLEDGE CTR OF DENMARK

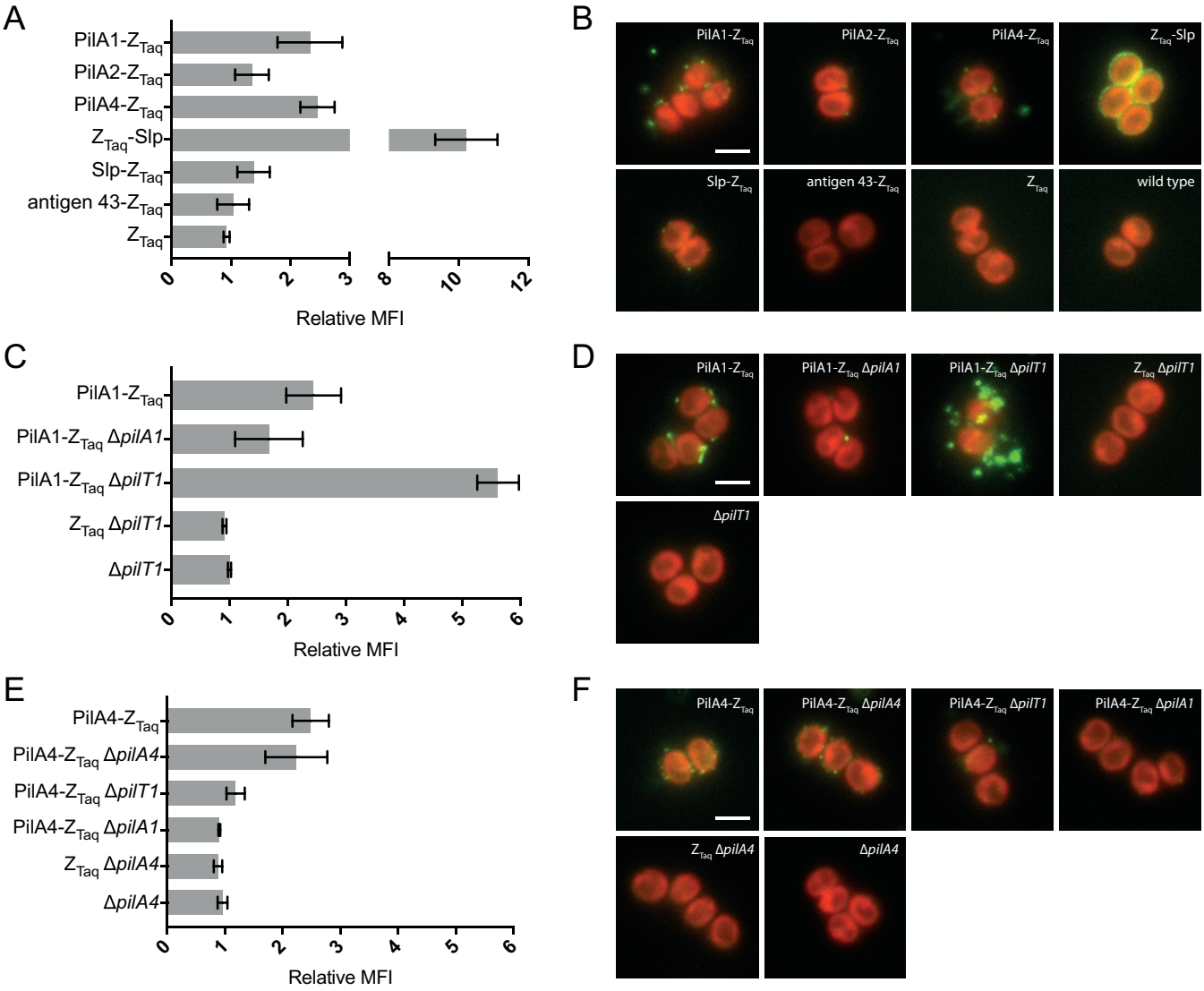

FIG 2 Detection of surface-displayed Z_{Taq} on *Synechocystis* cells via flow cytometry and immunofluorescence analysis. An antiaffibody antibody and a secondary antibody labeled with Alexa Fluor 488 were used for detection. For the flow cytometry analysis (A, C, and E), the obtained median fluorescence intensity (MFI) values were normalized to that of the wild-type control, resulting in relative MFI values. All flow cytometry data are presented as averages ± standard deviations from four independent experiments. For the immunofluorescence analysis (B, D, and F), representative images of labeled, if present, *Synechocystis* cells are shown. The cells were analyzed for autofluorescence (chlorophyll *a*) (Texas Red filter) and Z_{Taq} display (Alexa Fluor 488) (GFP filter) (bars, 2 μm). (A and B) Evaluation of Z_{Taq} display levels for all selected potential native (PilA1, PilA2, PilA4, and Slp) and heterologous (antigen 43) carrier proteins. A control expressing Z_{Taq} intracellularly was included. An additional wild-type control for immunofluorescence is shown. (C and D) Evaluation of Z_{Taq} display levels for PilA1-Z_{Taq} strains with knockouts of *pilA1* or *pilT1*. Controls (Z_{Taq} Δ*pilT1* and Δ*pilT1*) were also evaluated. (E and F) Evaluation of Z_{Taq} display levels for PilA4-Z_{Taq} strains with knockouts of *pilA4*, *pilT1*, or *pilA1*. Controls (Z_{Taq} Δ*pilA4* and Δ*pilA4*) were also evaluated.

addition, immunofluorescence analysis showed that the Z_{Taq}-Slp fusion proteins were able to assemble into cell-enveloping S-layer structures (Fig. 2B). The collected flow cytometry data were also analyzed in terms of the percentage of labeled, and, thus, Z_{Taq}-displaying, cells within the studied populations (see Fig. S1B and S1C in the supplemental material for an example of the gating procedure). Approximately 50% of the PilA1-Z_{Taq} and PilA4-Z_{Taq} cells and 95% of the Z_{Taq}-Slp cells displayed the affibody (Fig. S3A). While labeled cells were visible within the PilA2-Z_{Taq} and Slp-Z_{Taq} populations by immunofluorescence, the percentage of labeled cells, as determined by flow cytometry, was less than 5%. Collectively, these results show that C-terminal fusions to the pilin proteins PilA1 and PilA4, as well as N-terminal fusion to Slp, were able to mediate the most promising levels of functional display and extracellular availability of Z_{Taq}.

Downloaded from http://jb.asm.org/ on August 9, 2018 by TECH KNOWLEDGE CTR OF DENMARK

In common for PilA1, PilA4, and Slp is that they are confirmed or putative subunits of externally accessible structures of the cell (Fig. 1A). We speculated that the S-layer could form a physical barrier that hinders membrane-integrated antigen 43 to mediate the accessible display of Z_{Taq}; this was found to be the case for a porin-based display system in *S. elongatus* (17). However, later results showed that the wild-type *Synechocystis* strain used in this study lacks an external S-layer, most likely due to the identified 76-bp deletion in its gene, meaning that no possibly occluding S-layer was present. We conclude that antigen 43 was not able to display Z_{Taq} on the cell surface.

Improving Z_{Taq} display for the carrier proteins PilA1 and PilA4. We next attempted to improve the display efficiency of the PilA1-Z_{Taq} and PilA4-Z_{Taq} strains to levels similar to that of the Z_{Taq}-Slp strain. In an attempt to replace all native proteins with Z_{Taq} fusion variants, *pilA1* (*sll1694*) and *pilA4* (*slr1456*) gene knockouts were introduced into the respective strains. In addition, the knockout of *pilT1* (*slr0161*) was evaluated for both strains. PilT1 is an ATPase responsible for the retraction, by ATP-driven depolymerization, of type IV pili in *Synechocystis* (41). Disruption of *pilT1* yields a nonmotile and hyperpiliated phenotype (22, 41). This hyperpiliation could lead to an increase in the number of surface-exposed Z_{Taq} molecules when fused to pilus subunits.

A PilA1-Z_{Taq} Δ*pilA1* strain had reduced Z_{Taq} display (Fig. 2C and D), indicating that the presence of native PilA1 is required to uphold the functional assembly of the pilus structure. Δ*pilA1* and Z_{Taq} Δ*pilA1* controls were not included for analysis due to clumping during cultivation; this phenotype was described previously for Δ*pilA1* strains (23). Knockout of *pilT1* in the PilA1-Z_{Taq} Δ*pilT1* strain increased Z_{Taq} display more than 2-fold, as measured by relative MFI (Fig. 2C) and as seen by immunofluorescence (Fig. 2D). In addition, the micrographs of the PilA1-Z_{Taq} Δ*pilT1* strain showed cells surrounded by fluorescent extending bundles of pili (Fig. 2D; see also Fig. S2B in the supplemental material), supporting that pilus synthesis could take place while incorporating the fusion protein. The percentage of labeled and displaying cells within the PilA1-Z_{Taq} Δ*pilT1* population improved to 87% (Fig. S3B).

Disruption of *pilA4* in the PilA4-Z_{Taq} Δ*pilA4* strain did not affect Z_{Taq} display (Fig. 2E and F). Surprisingly, disruption of *pilT1* in the PilA4-Z_{Taq} Δ*pilT1* strain led to a nearly complete loss of Z_{Taq} display. The same effect was evident in the reduced number of labeled cells within the PilA4-Z_{Taq} Δ*pilT1* population (Fig. S3C). To evaluate if the extracellular display of the PilA4-Z_{Taq} protein is associated with the type IV pili, a knockout of *pilA1* was carried out. Deletion of the gene for this major pilin (*pilA1*) leads to the loss of type IV pili on *Synechocystis* (22, 23). The PilA4-Z_{Taq} Δ*pilA1* strain lost Z_{Taq} display (Fig. 2E and F and Fig. S3C), supporting that PilA4-Z_{Taq} and possibly, by extension, PilA4 are dependent on the major pilin PilA1 or functional type IV pilus assembly for extracellular availability. In several instances, the fluorescence in the micrographs for the PilA4-Z_{Taq} base strain was localized to pilus-like structures extending from the cells (Fig. S4), further supporting that PilA4-Z_{Taq} is directly incorporated into the pilus. In light of this, the contrasting results for *pilT1* disruption in the PilA1-Z_{Taq} and PilA4-Z_{Taq} base strains are unexpected, potentially indicating divergent regulation for PilA4 and PilA1.

Effect on pilus and S-layer assembly due to incorporation of Z_{Taq} fusion proteins. The two best-performing Z_{Taq} display systems (Z_{Taq}-Slp and PilA1-Z_{Taq} Δ*pilT1*) have been shown to allow the extracellular availability of the Z_{Taq} fusion proteins. Although these strains were able to incorporate fusion proteins into the relevant surface structures (Fig. 2B and D), it was unclear if this nevertheless contributed negatively to the stability and assembly of these structures. To study this, the relative extracellular protein amounts of these structures were quantified. Protein fractions from the cell surface and culture media of selected strains were isolated and analyzed by SDS-PAGE and immunoblotting against Z_{Taq}. Fractions containing the cell surface-associated pili were obtained by shearing the pili off the cells by vortexing, an established method for isolation of pili (42). S-layer surface fractions were isolated by

Downloaded from http://jb.asm.org/ on August 9, 2018 by TECH KNOWLEDGE CTR OF DENMARK

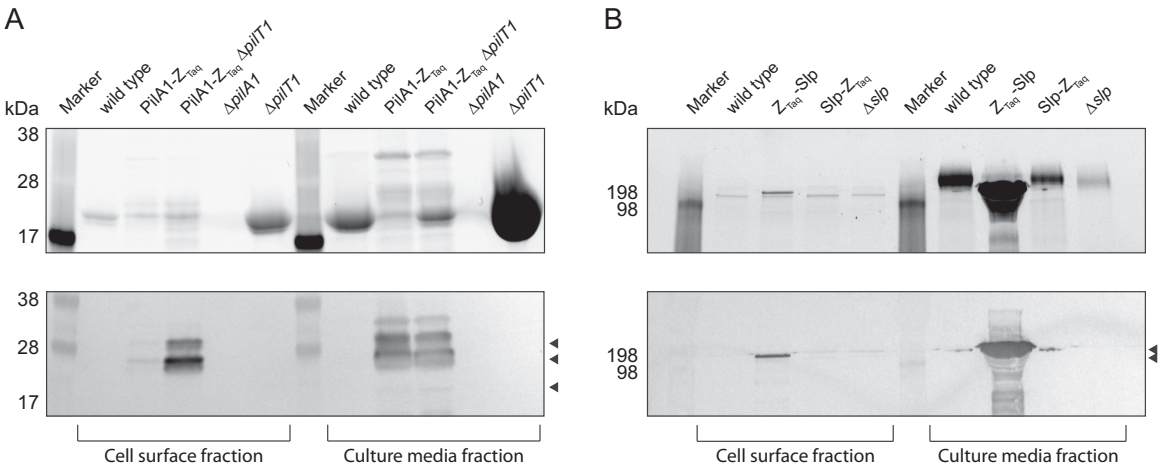

FIG 3 Amounts of pilin and S-layer proteins found on the cell surface or released into the culture medium for relevant Z_{Taq}-displaying *Synechocystis* strains. Surface fractions from equal amounts of cells, normalized by the OD_{730}, and the resulting normalized amounts of culture medium were analyzed by both SDS-PAGE (top images) and immunoblotting against Z_{Taq} (bottom images). Arrowheads denote expected sizes, as found for the whole-cell extract blots in Fig. 1E, for PilA1-Z_{Taq} or Z_{Taq}-Slp, respectively. (A) Analysis of the recoverable pilin protein amounts for PilA1-Z_{Taq}-expressing strains, in both wild-type and Δ*pilT1* strain backgrounds. Included controls are wild-type, Δ*pilA1*, and Δ*pilT1* strains. (B) Analysis of the recoverable S-layer protein amounts in strains expressing either Z_{Taq}-Slp or Slp-Z_{Taq}. Controls included are wild-type and Δ*slp* strains. For the medium fraction of Z_{Taq}-Slp, only one-sixth of the normalized amount was loaded due to the high protein concentration.

treating cells with EGTA, allowing the removal of the Ca^{2+} ions thought to stabilize the S-layer (34). In addition, the collected medium fractions were subjected to protein precipitation to concentrate any proteins shed off from the cells during cultivation.

Analysis of the pilin protein amounts showed that fewer pilins could be recovered from PilA1-Z_{Taq} than from the wild type (Fig. 3A). The PilA1-Z_{Taq} Δ*pilT1* strain allowed higher recovery of pilins than the base strain PilA1-Z_{Taq} (Fig. 3A), in agreement with the flow cytometry and immunofluorescence results (Fig. 2C and D); however, the amount of isolated pilins did not reach the same level as for the Δ*pilT1* background strain. The reduced amounts of extractable cell surface-associated pili in both PilA1-Z_{Taq}-expressing strains, compared to the amounts in their background strains, indicate that although type IV pilus synthesis was possible while incorporating the fusion proteins, it was also negatively affected by it. The immunofluorescence micrographs of the PilA1-Z_{Taq} base strain (Fig. 2B; see also Fig. S2A in the supplemental material) show fluorescence mainly close to the cell surface rather than in extending pilus-like structures. This indicates a potential truncation of the pili due to PilA1-Z_{Taq} incorporation, explaining the smaller amount of recovered extracellular pilins from these strains. The two control strains (Δ*pilA1* and Δ*pilT1*) showed, as expected, no recoverable pilins and hyperpiliation, respectively (Fig. 3A). The trends seen for the cell surface fractions were also seen for the medium fractions. The wild type itself shed large amounts of pilus subunits into the media. The amount of shed pilin proteins remained smaller in the PilA1-Z_{Taq}-expressing strains, further indicating that these strains had fewer or shorter pili available for shedding. Immunoblotting against Z_{Taq} confirmed that PilA1-Z_{Taq} fusion proteins were successfully incorporated into the recovered cell surface-associated pili (Fig. 3A). The correspondence of the bands on the blot with the larger expected sizes indicates that any extracellularly present PilA1-Z_{Taq} protein was post-translationally modified, although it is not known if these modifications are the same as for native PilA1 (38–40).

For comparison of the S-layer amounts, a Δ*slp* strain was included as a control to correctly identify the band belonging to Slp. However, the protein profiles for the wild-type and Δ*slp* strains did not differ (Fig. 3B). This indicates that the wild-type host used in this study lacks an S-layer, probably due to the identified 76-bp deletion in the middle of its Slp gene (*sll1951*). For the Z_{Taq}-Slp strain, the larger of the expected bands, presumably corresponding to the glycosylated protein (21), was present in the cell

Downloaded from http://jb.asm.org/ on August 9, 2018 by TECH KNOWLEDGE CTR OF DENMARK

surface fraction. This supports the above-described immunofluorescence data (Fig. 2B and Fig. S2A) and proves that the fusion proteins could correctly cross the cell wall of *Synechocystis* and assemble into an S-layer on the cell surface. However, the medium fraction for the same Z_{Taq}-Slp strain showed that large quantities of the fusion protein were also shed from the cell (Fig. 3B). Although some protein was found on the surface, the shedding suggests that anchoring of the protein was negatively affected by the N-terminal fusion of Z_{Taq}. In contrast, the Slp-Z_{Taq} strain had no detectable levels of extracellularly available fusion protein in the cell surface or medium fraction. This indicates that the C-terminal fusion of Z_{Taq} instead impaired the secretion of the protein.

Regardless of the Z_{Taq}-Slp strain being the best-performing display strain during flow cytometry (Fig. 2A), it was deemed unsuitable as a display system due to the high level of fusion protein shedding (Fig. 3B). Altogether, this meant that PilA1-Z_{Taq} expressed in a Δ*pilT1* background was the most stable surface display system. We examined this strain for growth and pilus-mediated functions such as cell motility and transformation competency. Growth of the PilA1-Z_{Taq} Δ*pilT1* strain was equal to the that of the wild type (Fig. S5A). Motility assays of a motile *Synechocystis* strain transformed to express PilA1-Z_{Taq} showed that this led to a loss of motility, thus exhibiting a dominant negative phenotype (Fig. S5B). The natural transformation efficiency of the PilA1-Z_{Taq} *Synechocystis* strain was also reduced; it retained less than 20% of the competency of the wild type (Fig. S5C). In summary, these results show that fusing Z_{Taq} to PilA1 impaired pilus-mediated functions; however, the detection of extracellular fusion proteins in pilus-like structures by immunofluorescence and in the extracted pilin fractions supports that pilus assembly was still able to progress to some degree. Comparison to the well-established *Staphylococcus carnosus* surface display system (43) showed that the display level for the *Synechocystis* PilA1-Z_{Taq} Δ*pilT1* strain was less than half that for a Z_{Taq}-displaying *S. carnosus* strain (Fig. S6) (44, 45).

Quantification of the relative amounts of Z_{Taq} fusion proteins in the sheared and shed pilus fractions from PilA4-Z_{Taq} *Synechocystis* strains. An improvement in the Z_{Taq} display level for the PilA4-Z_{Taq} base strain was not realized, as was managed for PilA1-Z_{Taq} in this study. However, successful affibody tagging of this putative minor pilin made the various constructed strains interesting to study. The amount of pilin proteins extractable from the cells or shed into the medium was assessed as described above for the PilA1-Z_{Taq} strains.

For the PilA4-Z_{Taq} and PilA4-Z_{Taq} Δ*pilA4* strains, smaller amounts of cell surface-associated pilins were recovered than for the wild type (Fig. 4). Immunoblotting against Z_{Taq} showed that PilA4-Z_{Taq} was found among the recovered pilin proteins. The observed band corresponded to the larger of the expected sizes, indicating that the extracellularly present PilA4-Z_{Taq} protein was posttranslationally modified. Knockout of *pilA1*, creating the PilA4-Z_{Taq} Δ*pilA1* strain, yielded no isolatable pilins or detectable PilA4-Z_{Taq} in either the surface or medium fraction, as expected. This supports the above-described data (Fig. 2C and D) and again suggests that the external availability of PilA4-Z_{Taq} depends on PilA1 due to incorporation into the type IV pili (see Fig. S4 in the supplemental material). Knockout of *pilT1*, creating the PilA4-Z_{Taq} Δ*pilT1* strain, increased the amount of recovered pilins from the cells and the amounts shed into the media, as expected (Fig. 4). However, regardless of this increased pilus availability, the signal for any present PilA4-Z_{Taq} was reduced in the immunoblot, suggesting that its extracellular presence is also potentially associated with PilT1. In addition, the increased shedding of pili into the media for the Δ*pilA4* strain indicates that PilA4 is involved in the retraction or stability of type IV pili in *Synechocystis*.

Due to the presumed incorporation of PilA4-Z_{Taq} into the type IV pili, its effect on pilus-associated motility and transformation competency was analyzed as was done for PilA1-Z_{Taq}. The expression of PilA4-Z_{Taq} in a motile *Synechocystis* strain did not negatively affect motility (Fig. S5B); it was previously shown that a deletion of *pilA4* has no effect on motility (23). However, the transformation efficiency of the PilA4-Z_{Taq} strain was reduced by more than 80% compared to the wild type (Fig. S5C).

Downloaded from http://jb.asm.org/ on August 9, 2018 by TECH KNOWLEDGE CTR OF DENMARK

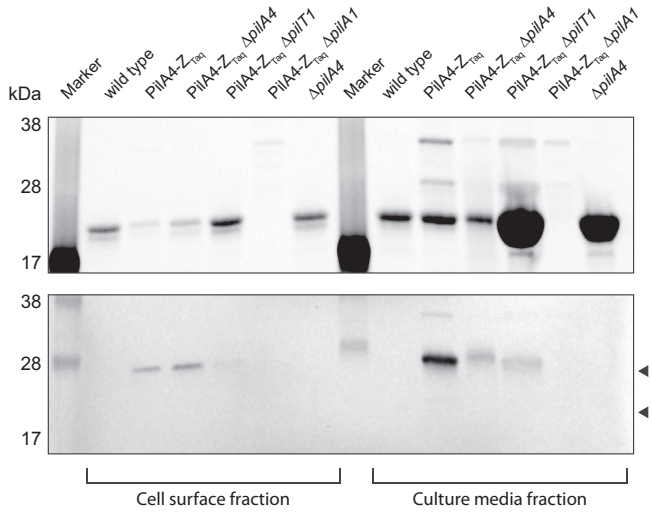

FIG 4 Analysis of various PilA4-Z_{Taq}-expressing *Synechocystis* strains for their amounts of recoverable cell surface-associated and released pilins. Surface fractions from equal amounts of cells, normalized by the OD_{730}, and the resulting normalized amounts of culture medium were analyzed by both SDS-PAGE (top) and immunoblotting against Z_{Taq} (bottom). PilA4-Z_{Taq}-expressing strains in wild-type, Δ*pilA4*, Δ*pilT1*, and Δ*pilA1* strain backgrounds were evaluated. A Δ*pilA4* control was also included. Arrowheads denote the expected sizes for the PilA4-Z_{Taq} protein, as found for the whole-cell extract blot in Fig. 1E.

Display of polymerizing affibodies for affinity-driven *Synechocystis* aggregation. Display of complex-forming affibodies on different strains of *Synechocystis* could be used to mediate cell-cell binding. An anti-idiotypic affibody to Z_{Taq} (antiZ_{Taq}) has been isolated; this Z_{Taq}:antiZ_{Taq} pair has a dissociation constant of 0.7 μM (46). A *Synechocystis* strain displaying antiZ_{Taq} was constructed by using the established display system, creating the PilA1-antiZ_{Taq} Δ*pilT1* strain. Display of antiZ_{Taq} was confirmed by flow cytometry and immunofluorescence and was found be improved compared to that for the PilA1-Z_{Taq} Δ*pilT1* strain (see Fig. S7 in the supplemental material). Mixing *Synechocystis* strains expressing Z_{Taq} or antiZ_{Taq} could allow cells of the different strains to bind together due to Z_{Taq}:antiZ_{Taq} complex formation. It was hypothesized that such binding could drive floc formation and thus improve sedimentation; this could in turn benefit biomass collection.

Cell suspensions, consisting of individual strains or mixes thereof, were evaluated in terms of sedimentation speeds of the biomass. For individual strains, it was clear that the cells of all modified strains settled faster than the wild-type control (Fig. 5A). The PilA1-Z_{Taq} and PilA1-antiZ_{Taq} strains were the quickest to settle. Deletion of *pilT1* in these strains slowed their sedimentation speeds, suggesting that the increased piliation associated with this genotype has a positive effect on cell buoyancy. Such a correlation between piliation and buoyancy was suggested in other studies previously (47, 48).

To test if a mix of Z_{Taq}- and antiZ_{Taq}-displaying *Synechocystis* strains could lead to affibody-driven aggregation, the PilA1-Z_{Taq} Δ*pilT1* and PilA1-antiZ_{Taq} Δ*pilT1* strains were mixed together. A mixture of the PilA1-Z_{Taq} Δ*pilT1* and PilA1-Z_{Taq} strains was tested in parallel as a control. For the latter pair, the two strains should not interact due to the display of the same affibody (Z_{Taq}). Any improvement in sedimentation for this pair is rather a result of sweeping, by the fast sedimenter PilA1-Z_{Taq}, than due to interaction. Sedimentation rates were equal for both mixtures (Fig. 5B), indicating that the interactions between Z_{Taq} and antiZ_{Taq} were too weak or too few to induce stable floc formation. To assess if minor interactions occurred, which would not result in drastic flocculation, the above-described strain mixtures were also analyzed by phase-contrast microscopy. Samples were taken 4 h into the sedimentation test. The sizes of all aggregates in the resulting micrographs, including all single cells and multicellular aggregates, were analyzed by using Fiji (ImageJ) (49). For an example of the procedure, see Fig. S8A and S8B in the supplemental material. No significant size differences could

Downloaded from http://jb.asm.org/ on August 9, 2018 by TECH KNOWLEDGE CTR OF DENMARK

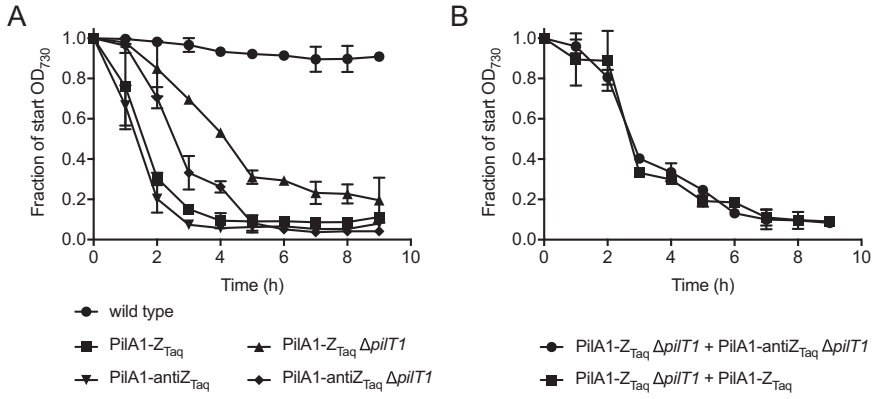

FIG 5 Analysis of sedimentation speeds for *Synechocystis* strains displaying affibodies. (A) Sedimentation of individual strains of *Synechocystis* displaying either Z_{Taq} or the anti-idiotype affibody antiZ$_{Taq}$ through fusion to PilA1, in a wild-type or Δ*pilT1* background. (B) Sedimentation of mixtures of *Synechocystis* strains expressing complementary affibodies (PilA1-Z_{Taq} Δ*pilT1* and PilA1-antiZ$_{Taq}$ Δ*pilT1*) or the same affibody (PilA1-Z_{Taq} Δ*pilT1* and PilA1-Z_{Taq}). All data are presented as averages ± standard deviations from two independent experiments. Nonvisible error bars are smaller than the data symbol.

be observed between aggregates from the two mixtures or compared to the single strains (Fig. S8C), demonstrating a lack of specific interactions between the cells of the Z_{Taq} and antiZ$_{Taq}$ strains.

Previous studies have shown that the time of contact between interacting partners is an important parameter to consider (50). To test this, the PilA1-Z_{Taq} Δ*pilT1* and PilA1-antiZ$_{Taq}$ Δ*pilT1* strains were cultivated together and then analyzed for improved sedimentation, in comparison to the strains grown individually. Phase-contrast microscopy was again used to identify more discrete cell aggregation. However, no improvements in either parameter were observed (data not shown).

Display of polymerizing affibodies to mediate interspecies cell-cell binding. The display of complementary affibodies was also assessed for enabling binding between *Synechocystis* and the heterotrophic bacterium *E. coli* or *S. carnosus*. Both of these bacteria have established surface display systems: *E. coli* display is based on the adhesin involved in diffuse adherence (AIDA-I) autotransporter (45), while *S. carnosus* display is based on the cell wall-anchoring region of *Staphylococcus aureus* protein A (43, 51). The *E. coli* and *S. carnosus* display constructs contain the streptococcal protein G albumin binding domain (ABD) (5.1 kDa) and albumin binding protein (ABP) (21.8 kDa) as spacers, respectively (52). Both ABD and ABP are useful targets for fluorescein isothiocyanate (FITC)-tagged human serum albumin (HSA), to serve as a marker for the level of surface expression in these hosts (53).

E. coli strains displaying Z_{Taq} or antiZ$_{Taq}$ were constructed by using the AIDA-I system (45); however, a minimized version of the previously reported vector was used (54). *S. carnosus* strains displaying the same affibodies were received as gifts from John Löfblom (KTH School of Biotechnology, Sweden). Labeling of strains with FITC-tagged HSA showed that roughly 100% of the *E. coli* cells and 84% of the *S. carnosus* cells were labeled and thus displayed affibodies (see Fig. S9A in the supplemental material). Analysis of the subpopulations of labeled cells further showed that the level of surface expression was higher and more evenly distributed on the cells for *E. coli* than for *S. carnosus* (Fig. S9B to D).

Interactions between affibody-displaying *Synechocystis* and *E. coli* or *S. carnosus* displaying either Z_{Taq} or antiZ$_{Taq}$ was tested by incubating a mix of cells and analyzing interactions via flow cytometry. In these assays, *Synechocystis* was discriminated by its phycocyanin autofluorescence (channel FL6; emission at 640 nm and excitation at 620 nm), and *E. coli* or *S. carnosus* was discriminated by being labeled with FITC-tagged HSA (channel FL1; emission at 525 nm and excitation at 488 nm). An event having fluorescence in both channels suggested a *Synechocystis*-*E. coli* or *Synechocystis*-*S. carnosus*

Downloaded from http://jb.asm.org/ on August 9, 2018 by TECH KNOWLEDGE CTR OF DENMARK

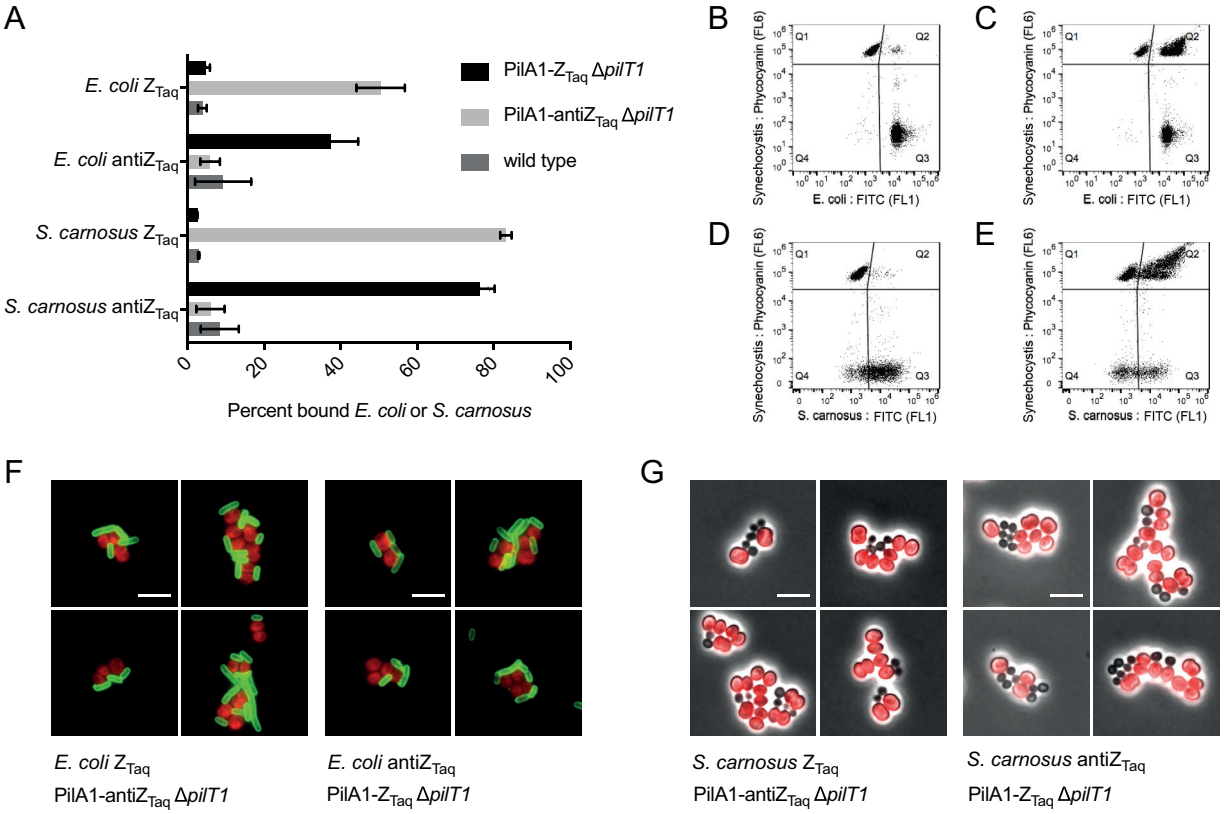

FIG 6 Flow cytometry and microscopy analysis to assess the level and nature of cell-cell binding between *Synechocystis* and *E. coli* or *S. carnosus*, driven by complex formation of surface-displayed complementary affibodies. (A) Flow cytometry was used to test three *Synechocystis* strains (PilA1-Z_{Taq} Δ*pilT1*, PilA1-antiZ_{Taq} Δ*pilT1*, and the wild type) for their ability to bind to *E. coli* or *S. carnosus* displaying either Z_{Taq} or antiZ_{Taq}. The level of interaction is presented as the percentage of FITC-labeled *E. coli* or *S. carnosus* cells found in Q2 (signal registered in both the FL1 and FL6 channels), as opposed to the total number of labeled cells (Q2 and Q3). All data are presented as averages ± standard deviations from three independent experiments. (B and C) Representative quadrant plots for the analyzed interactions between FITC-labeled *E. coli* Z_{Taq} and *Synechocystis* wild-type (B) or PilA1-antiZ_{Taq} Δ*pilT1* (C) strains. (D and E) Representative quadrant plots for the analyzed interactions between FITC-labeled *S. carnosus* Z_{Taq} and *Synechocystis* wild-type (D) or PilA1-antiZ_{Taq} Δ*pilT1* (E) strains. (F) Representative micrographs of cell-cell binding between *E. coli* and *Synechocystis*. Shown are overlays of cyanobacterial autofluorescence (Texas Red filter) and FITC-labeled *E. coli* (GFP filter). (G) Representative micrographs of cell-cell binding between *S. carnosus* and *Synechocystis*. Shown are overlays of cyanobacterial autofluorescence (Texas Red filter) and phase-contrast images (bars, 5 μm).

complex. The cytometry data were visualized in quadrant plots, where only FL6-positive events ended up in quadrant 1 (Q1), only FL1-positive events were found in Q3, and both FL6- and FL1-positive events, which indicate an interaction, were registered in Q2. Unlabeled *E. coli* and *S. carnosus* ended up in Q4. Interactions were quantified by calculating the percentage of labeled *E. coli* or *S. carnosus* cells found in Q2.

Interactions between *Synechocystis* and *E. coli* or *S. carnosus* expressing complementary affibodies were evident, showing that the Z_{Taq}:antiZ_{Taq} complex could successfully form between mixed cells (Fig. 6A). The lack of an interaction with wild-type *Synechocystis* cells or between cells expressing the same affibody proves the specificity of binding between cells. The percentage of *S. carnosus* cells binding to cyanobacteria was higher than that for *E. coli* (Fig. 6A), even though the *E. coli* cells had a higher display level than *S. carnosus* (Fig. S9B). This could be due to the larger ABP spacer on *S. carnosus*, thus allowing greater accessibility to the displayed affibodies. The display level proved more important for the different *Synechocystis* strains. The PilA1-antiZ_{Taq} Δ*pilT1* strain, which had the highest display level (Fig. S7A), also managed to bind to a higher percentage of Z_{Taq}-displaying *E. coli* or *S. carnosus* cells than the PilA1-Z_{Taq} Δ*pilT1* strain to its counterparts (Fig. 6A). Representative quadrant plots showing successful events of binding between *E. coli* or *S. carnosus* and *Synechocystis* are shown in Fig. 6C and E, respectively. These plots can be compared to plots where no

Downloaded from http://jb.asm.org/ on August 9, 2018 by TECH KNOWLEDGE CTR OF DENMARK

interaction was evident due to wild-type *Synechocystis* being tested as an interaction partner (Fig. 6B and D).

The nature of the cell-cell binding between *Synechocystis* and *E. coli* or *S. carnosus* was further studied by microscopy. *Synechocystis* was identified by its phycocyanin autofluorescence (Texas Red filter), as in the flow cytometry analysis. The *E. coli* and *S. carnosus* strains were again labeled with FITC-tagged HSA (green fluorescent protein [GFP] filter); however, due to the uneven labeling of *S. carnosus* cells (Fig. S9D), this method of identification was used only for *E. coli* (Fig. 6F). The *S. carnosus* cells were instead identified by their smaller size and darker color in the phase-contrast images (Fig. 6G). More representative micrographs, in addition to the ones shown in Fig. 6F and G, can be seen in Fig. S10 in the supplemental material. Both large and small groups of aggregated cells could be found in the micrographs (Fig. 6F and G and Fig. S10). However, smaller groups consisting of a few cells of each microbe type predominated. The largest groups were found for binding between *Synechocystis* and *S. carnosus* (Fig. 6G and Fig. S10B), reflecting the higher level of binding for *S. carnosus* than for *E. coli* in the flow cytometry analysis. Interactions between the different species showcased a higher degree of distinctly confined species groups upon interactions with *S. carnosus* (Fig. 6G and Fig. S10B), while a higher degree of dispersal for the interacting species was seen for interactions with *E. coli* (Fig. 6F and Fig. S10A).

DISCUSSION

Our findings demonstrate that C-terminal fusions to the major type IV pilin protein PilA1 can be used for surface display purposes in *Synechocystis*. Display was improved by knocking out the gene encoding PilT1, the ATPase responsible for pilus retraction. This is, to our knowledge, the first example of the surface display of a heterologous protein on *Synechocystis* driven by fusion to a native surface structure. The incorporation of PilA1-Z_{Taq} fusion proteins into the type IV pili still allowed some degree of pilus assembly; however, pilus-associated functions, such as motility and natural competency, were negatively affected. Display of proteins larger than affibodies (6.5 kDa) may not be possible since these proteins may hinder the correct assembly of the pilus. Possible limitations regarding passenger size were noted previously for surface display by fusion to pilus or fimbria subunits (55). Regardless, display by fusion to these subunits is attractive due to the high number of these structures present on the cell surface.

Complex-forming affibody pairs have recently been used to colocalize biosynthetic enzymes in metabolic pathways (56). Here, it was shown that the same principle could be applied for driving cell-cell binding. *Synechocystis* strains and *E. coli* or *S. carnosus* strains expressing complementary affibodies bound specifically to each other. This has implications for future photosynthetic microbial communities. One such application could be to physically bind heterotrophs to cyanobacteria that have been modified to produce and secrete feedstocks such as sugars (57), acetate (3), or glycerol (58). This forced proximity could allow a more efficient chemical transfer between microbes than what could be realized in a free-floating setup. Similar interspecies binding between FLAG-displaying *S. elongatus* and protein A-displaying *S. cerevisiae* has also been shown (17). However, in that system, an externally added antibody was necessary to bring the cells together. Attachment between the cyanobacterium *Microcystis aeruginosa* and an *E. coli* strain engineered to display a cyanobacterial lectin has also been described (59).

The inability to induce flocculation and improve sedimentation for a mixture of *Synechocystis* strains displaying complementary affibodies could be because the display level of the Z_{Taq}:antiZ_{Taq} complex was not high enough to drive cell-cell binding. The display level for the PilA1-Z_{Taq} Δ*pilT1 Synechocystis* strain was shown to be less than half that for the Z_{Taq} display in *S. carnosus*; additionally, the *E. coli* AIDA-I system was previously shown to outperform affibody display in *S. carnosus* (45). This could explain why intraspecies *Synechocystis* binding did not occur, while interspecies binding with either *E. coli* or *S. carnosus* was possible. An improved display level in combination with other higher-affinity binding pairs could potentially overcome this. However, all tested

Downloaded from http://jb.asm.org/ on August 9, 2018 by TECH KNOWLEDGE CTR OF DENMARK

modified *Synechocystis* strains sedimented faster than the wild type. This could be due to the observed reduction in extractable pili from these strains and the potentially truncated nature of these pili due to the incorporation of fusion proteins. A positive correlation between cyanobacterial buoyancy and the presence and amount of pili was speculated previously (47, 48). The type IV pili in *Synechocystis* are also known to be glycosylated (39); such extracellular polysaccharides contribute to the overall negative charge of the cells, which allows them to remain in suspension (60). Reduced piliation of the cells would therefore also reduce the quantity of extracellular polysaccharides, possibly affecting the ability of the cells to remain suspended. The altered properties of the pili due to the incorporation of affibodies could also have played a role in affecting the buoyancy of the cells.

The described PilA1 display system in *Synechocystis* could also be extended to display peptides with affinities for different types of materials (61, 62), facilitating, e.g., cell immobilization. This could aid in the use of cyanobacteria in large-scale processes.

Our results can also be used to further understand the type IV pili in *Synechocystis*. The location and function of the putative minor pilin PilA4 in *Synechocystis* are, to our knowledge, so far unknown. Previous studies have shown that PilA4 is not essential for type IV pilus-driven motility in *Synechocystis* (23), and here, the expression of PilA4-Z_{Taq} did not affect motility. Its function as a carrier protein in this study shows that PilA4 locates to the surface of the cell. The inability of PilA4-Z_{Taq} to mediate display in a *pilA1* knockout strain, in addition to several instances of fluorescence being seen in pilus-like structures in immunofluorescence micrographs, further suggests that it is incorporated into the pilus. Knockout of the pilus retraction ATPase (*pilT1*) increased the display efficiency for PilA1-Z_{Taq} but caused an unexpected loss of display in the PilA4-Z_{Taq} strain. These contrasting results suggest divergent regulation or a different role for PilA4 than for PilA1. The reduced relative quantity of PilA4-Z_{Taq} in the pilin fraction upon PilT1 deletion, as well as the increased shedding of pilins in a Δ*pilA4* strain, indicates that PilA4 is a minor pilin involved in pilus retraction or stability while not being strictly required for pilus synthesis. However, more detailed studies are required in order to confidently confirm these suggestions. Minor pilins of type IV pilus systems in other organisms, such as *P. aeruginosa* and *Neisseria* spp., have mainly been implicated in priming the pilus for assembly rather than retraction (63–66). However, in the simpler *Vibrio cholerae* type IV pilus system, a minor pilin (TcpB) has been shown to act in both the assembly and retraction of pili (67). Similar affibody tagging of other putative minor pilins in *Synechocystis* could help elucidate their localization as well. For the other putative pilin included in this study, PilA2, immunofluorescence for the PilA2-Z_{Taq} protein was found to be located at the cell surface, indicating that this is the native location of PilA2. It is also important to note that the main *Synechocystis* host used in this study is nonmotile due to a mutation in the *spkA* gene (68). The characteristics of the pili for this nonmotile host could be different from those for a motile strain; reduced piliation for a nonmotile glucose-tolerant strain was noted previously (69). These possible differences mean that the above-noted results for the putative minor pilins may be different in the presence of a fully functional type IV pilus system.

Our results also clarify some aspects of the protein constituent of the *Synechocystis* S-layer. Blocking the C terminus of Slp by fusion to Z_{Taq} to a large extent hindered the correct secretion of the protein, supporting the notion that Slp carries a noncleavable C-terminal secretion signal, as was proposed previously (32, 34). In addition, fusion of Z_{Taq} to its N terminus allowed secretion and assembly into an S-layer but also resulted in excessive shedding of the fusion protein into the culture medium. This indicates that the region responsible for the surface anchoring of Slp is located in the N-terminal part of the protein. These effects have also been observed when the S-layer protein (RsaA) in *Caulobacter crescentus* was used for the surface display of fused peptides (70). The ability to identify permissive sites within RsaA, suitable for the surface display of passengers of various sizes (71), indicates that the same could be done for Slp from *Synechocystis*.

In conclusion, this work demonstrates the ability to successfully display an affibody

Downloaded from http://jb.asm.org/ on August 9, 2018 by TECH KNOWLEDGE CTR OF DENMARK

passenger protein on the cell surface of *Synechocystis* by fusion to PilA1, the major pilin protein of the native type IV pili. Affibody-displaying *Synechocystis* strains were able to bind by protein complex formation to *E. coli* or *S. carnosus* strains displaying the anti-idiotypic affibodies. These results have implications for the development of methods that would enable the immobilization of *Synechocystis* onto surfaces or other microbes in engineered microbial consortia. In addition, the putative minor pilin PilA4 was shown to localize to the cell surface in a presumably type IV pilus-dependent manner, and the protein domains responsible for the secretion and anchoring of the S-layer protein in *Synechocystis* were proposed to be located at the C and N termini, respectively.

MATERIALS AND METHODS

Culture conditions. Wild-type *Synechocystis* sp. strain PCC 6803 (a gift from Martin Fulda, University of Gottingen, Germany) used in this study is a nonmotile GT-S derivative. *Synechocystis* strains were cultivated in BG11 medium buffered to pH 7.9 with 25 mM HEPES. Cultures were grown in a climatic chamber (catalog number SE-1100; Percival Climatics) at 30°C with 20 μE/s/m^2 illumination and 1% (vol/vol) CO_2. For growth on solid medium, 1.5% (wt/vol) agar and 0.3% (wt/vol) sodium thiosulfate were added to BG11 medium. When needed, antibiotics were added (50 μg/ml kanamycin, 25 μg/ml chloramphenicol, and 50 μg/ml spectinomycin). Unless noted otherwise, cells were cultivated in 24-deep-well plates on a Multi-Genie microplate shaker. The plates were sealed by using sterile gas-permeable adhesive seals. The sides of the plates were covered with aluminum foil to allow equal light supply, from above, to all wells. Growth was monitored by measuring the optical density at 730 nm (OD_{730}).

S. carnosus strains (gifts from John Löfblom, KTH School of Biotechnology, Sweden) and *E. coli* strains were cultivated at 37°C in chloramphenicol-supplemented B2 and LB media, respectively.

Plasmid and strain construction. All strains and plasmids used in this study are described in Table 1. All primers are listed in Table S1 in the supplemental material.

The replicative plasmid pJA2 was used for expressing fusion proteins in *Synechocystis* under the control of the P_{psbA2} promoter (30). This replicative plasmid originates from the pPMQAK1 vector constructed previously by Huang et al. (72), which was subsequently modified by Anfelt et al. (26). To prepare the pJA2 backbone, it was PCR amplified, treated with DpnI, digested with XbaI and PstI (or AvrII and SpeI), and subjected to FastAP thermosensitive alkaline phosphatase.

Amplification of affibody genes (see the supplemental material for sequences) and carrier protein genes was done by introducing a flexible linker region (GSSSGSS) and restriction enzyme sites at either end. *pilA1* (*sll1694*), *pilA2* (*sll1695*), *pilA4* (*sll1456*), and the S-layer protein gene (*sll1951*) were amplified from purified *Synechocystis* genomic DNA. Amplification of *sll1951* required touchdown PCR (73). The fusion protein genes were constructed with overlap PCR, where the complementary linker sequence was used to enable fragment fusion. Cloning into the pJA2 vector was achieved via restriction enzyme digestion, ligation, and subcloning into *E. coli*.

The antigen 43 autotransporter construct required amplification of the signal peptide (amino acids 1 to 52) and β-chain translocator domain (amino acids 552 to 1039) from the *flu* gene of *E. coli* Top10. The affibody gene was fused to the β-chain domain fragment via overlap PCR. The signal peptide was added by subcloning in *E. coli*. The full insert was finally cloned into the pJA2 backbone.

The Golden Gate method (74), using the GeneArt Typells assembly kit (AarI), was used to construct suicide vectors for creating gene knockouts in *Synechocystis*.

The constructed replicative pJA2 plasmids were transformed into *Synechocystis* by electroporation. Suicide vectors were transformed into *Synechocystis* by natural transformation (75).

To enable AIDA-I-driven surface display of affibodies in *E. coli*, a minimized variant of the previously described pAraBAD-Z-EC vector (45), here called pAraBADmin, was used (this was a gift from Ken Andersson, KTH School of Biotechnology, Sweden). This variant has been minimized by 338 amino acids, mainly by exchanging the albumin binding protein for a smaller albumin binding domain and shortening the linker region between the passenger and the AIDA-I β-domain (54). This vector was digested with XhoI and SpeI, and equally digested affibody fragments were ligated into the backbone. Expression was done by using the *E. coli* BL21(DE3) strain.

***Synechocystis* cell lysis and immunoblotting against affibody fusion proteins.** Ten milliliters of cultures at an OD_{730} of 1 to 2 was pelleted and lysed in 400 μl lysis buffer consisting of 50 mM Tris-HCl, 150 mM NaCl, 1% Triton X-100, 1 mg/ml lysozyme, and complete EDTA-free protease inhibitor (Roche). The cells were incubated for 30 min at 37°C. Subsequently, 100 μl acid-washed glass beads was added, and bead beating was performed by vigorous shaking for 20 min at 4°C. Lysates were collected by centrifugation. Twenty micrograms of total protein per sample was analyzed by using SDS-PAGE, by transfer onto a 0.45-μm polyvinylidene difluoride (PVDF) membrane. Immunoblotting was done by using all solutions, except for the secondary antibody, provided in the WesternBreeze chromogenic kit. As a primary antibody, a goat antiaffibody antibody (Affibody AB) was used at 0.1 μg/ml. A secondary anti-goat alkaline phosphatase-conjugated antibody (catalog number A4187; Sigma) was used at a 1:10,000 dilution.

Prediction of signal peptides was done for all carriers and taken into account when calculating expected protein sizes. PILFIND 1.0 (76) was used for PilA1, PilA2, and PilA4. No cleavable signal peptide was detected for the S-layer protein. The signal peptide for *E. coli* antigen 43 is known (77).

Downloaded from http://jb.asm.org/ on August 9, 2018 by TECH KNOWLEDGE CTR OF DENMARK

Flow cytometry to assess affibody surface display on *Synechocystis*. Cells were analyzed after 50 h of growth, at an OD_{730} of 2.5 to 3. Fifty microliters of each culture was pelleted, and the cells were washed twice with PBS-P (phosphate-buffered saline supplemented with 0.1% [wt/vol] Pluronic-F108NF [BASF Corporation, Mount Olive, NJ]). Cells were resuspended in 100 μl PBS-P containing 0.5 μg/ml goat antiaffibody antibody (Affibody AB). Incubation was done at room temperature (RT) with slow mixing for 1 h. Afterwards, cells were pelleted, washed once in PBS-P, and then resuspended in 100 μl PBS-P containing 0.5 μg/ml anti-goat Alexa Fluor 488-conjugated antibody (Life Technologies). Incubation was carried out in the dark for 1 h on ice. Cells were again pelleted and washed once in PBS-P. Finally, the cells were resuspended in PBS-P, and fluorescence was measured by flow cytometry (Beckman Gallios; Beckman Coulter) using channel FL1 (emission at 525 nm and excitation at 488 nm). A total of 10,000 events were acquired. Data analysis was done by using FlowJo (FlowJo LLC). The cell population was gated based on the samples' front-scatter (FSC)-versus-side-scatter (SSC) dot plot. The gated cells were analyzed for their median fluorescence intensity (MFI) within the FL1 channel. All mutant strain MFI values were normalized against the MFI measured for the wild-type control in each run; the results are thus presented as relative values.

Relative quantification of pilus and S-layer protein amounts on the cell surface and in culture media. *Synechocystis* strains were grown in shake flasks until the OD_{730} reached ~2. Normalized amounts, by using the OD_{730} values, were pelleted; 50 ml was used for the most-dilute culture. Both the cell pellet and resulting culture medium were saved for further treatment.

For analysis of proteins in the culture medium, an adjusted version of a previously reported protocol was used (25). The medium was centrifuged three times to ensure the full removal of cells. Proteins were precipitated by the addition of trichloroacetic acid to a final concentration of 10% (wt/vol), incubation on ice for 2 h, and centrifugation for 15 min at 4°C. The protein pellet was washed twice in cold 90% acetone, dried, and resuspended in 1× loading buffer.

For the isolation of pili, the cell pellet was resuspended in 0.5 ml BG11 medium and vortexed for 5 min on the maximum setting. The suspension was centrifuged at 13,000 × *g*; this was repeated twice to fully remove all cells. The collected liquid fraction was further precipitated with trichloroacetic acid as described above for the culture medium. This protocol was adjusted from a previously described one (78).

For the isolation of S-layer proteins, the cell pellet was first washed in BG11 medium and then resuspended in 200 μl 10 mM HEPES containing 10 mM EGTA (pH 7.7) and incubated for 30 min at RT. Afterwards, the samples were vortexed for 2 min. The collected suspension was centrifuged at 13,000 × *g*; this was repeated twice to fully remove all cells. This protocol was adjusted from a previously described one (79).

SDS-PAGE and immunoblotting (see above for details) were performed on equal amounts of isolated fractions from all strains. The only exception to this was for the medium fraction from the Z_{Taq}-Slp strain, where only one-sixth of the amount was loaded.

Sedimentation assay of affibody-displaying *Synechocystis*. Cultures grown for 48 h, reaching an OD_{730} of ~2, were pelleted and resuspended in fresh BG11 medium to reach an OD_{730} of 2.5. Cells were transferred, as either single strains or a 1:1 mix of two strains, into glass tubes. Sedimentation rates were estimated by continuously measuring the OD_{730} of the topmost layer of the cell suspension.

Binding assay for affibody-displaying *Synechocystis* and *S. carnosus* or *E. coli*. Cultures of affibody-displaying *E. coli* grown overnight were diluted 100-fold into fresh LB medium and allowed to grow at 37°C until an OD_{600} of 0.5 was reached. Expression of the AIDA-I–affibody constructs was induced with 0.6% L-arabinose and subsequent cultivation for 3 h at 30°C (45). Affibody-displaying *S. carnosus* did not require induction. A total of 7.5 μl of *S. carnosus* cultures grown overnight or induced *E. coli* cultures grown as described above was taken for each sample. The cells were washed twice in PBS-P and labeled by incubation in PBS-P containing 225 nM FITC-labeled human serum albumin (HSA) for 1 h on ice. The cells were washed once after labeling in PBS-P. FITC-labeled HSA was prepared by labeling HSA using the Pierce NHS-fluorescein antibody labeling kit (Thermo Scientific) according to the supplier's recommendations.

To prepare the cyanobacterial cells, 50 μl of culture reaching an OD_{730} of ~3 was taken for each sample. The cells were washed twice in PBS-P.

The interaction assay mixtures were prepared by mixing washed *Synechocystis* cells and FITC-labeled *S. carnosus* or *E. coli* cells at a roughly equal ratio, to a total volume of 100 μl. The mixtures were incubated on ice for 2 h. Flow cytometry analysis was preceded by gently suspending the mixtures in PBS-P. Flow cytometry (Beckman Gallios; Beckman Coulter) analysis was done by registering events in channels FL1 (emission at 525 nm and excitation at 488 nm) and FL6 (emission at 640 nm and excitation at 620 nm). A total of 35,000 events were acquired. Data analysis was done by using FlowJo (FlowJo LLC). The cell populations were gated based on the samples' FSC-versus-SSC dot plots. The gated cells were analyzed in quadrant plots, where the signals obtained in channels FL6 (phycocyanin) and FL1 (FITC) were plotted for each event.

Microscopy and image analysis. Cells analyzed for the surface display of affibodies or interspecies cell-cell binding were prepared in the same manner as described above for flow cytometry analysis. Samples for analysis of intraspecies cyanobacterial binding were taken 4 h into the sedimentation test, done as described above. All samples were mounted onto 1% agarose pads prior to analysis. The mounted samples for the inter- and intraspecies binding tests were highly diluted to ensure that any observed aggregates were due to binding rather than a too-concentrated sample. A T*i* Eclipse inverted research microscope (Nikon) with a ×100/1.45-numerical-aperture (NA) objective (Nikon) was used to obtain phase-contrast and fluorescence images (GFP and Texas Red filters). Fiji (ImageJ) was used for image processing and analysis (49).

For the evaluation of intraspecies cyanobacterial binding, large-scale phase-contrast images were acquired by using the image stitching function of NIS-Elements microscopy software. These micrographs

Downloaded from http://jb.asm.org/ on August 9, 2018 by TECH KNOWLEDGE CTR OF DENMARK

were treated in Fiji with the "analyze particles" function to measure the size of all present aggregates, including single cells and multicellular aggregates. All noncell targets included by the software in the resulting data were manually removed.

SUPPLEMENTAL MATERIAL

Supplemental material for this article may be found at https://doi.org/10.1128/JB.00270-18.

SUPPLEMENTAL FILE 1, PDF file, 7.1 MB.

ACKNOWLEDGMENTS

This work was supported by the Swedish Foundation for Strategic Research (SSF) (RBP14-0013) and by a Science for Life Laboratory fellowship (B-2013-0201 to E.P.H.).

We thank John Löfblom for providing the *S. carnosus* strains used in the study, Anna-Luisa Volk for kindly giving an aliquot of the antiaffibody antibody, Ken Andersson for providing the minimized pAraBAD-Z-EC vector used for constructing the *E. coli* strains, Lun Yao for providing the pMD19-Δ*psbA1*::Sp^r vector, and Frederic D. Schramm for critical reading of the manuscript. We also thank the Jonas laboratory (Science for Life Laboratory, Stockholm University) for allowing us to use their microscope and Kristina Heinrich for help to set up the microscopy analysis.

We declare no conflicts of interest.

REFERENCES

1. Savakis P, Hellingwerf KJ. 2015. Engineering cyanobacteria for direct biofuel production from CO2. Curr Opin Biotechnol 33:8–14. https://doi.org/10.1016/j.copbio.2014.09.007.
2. Case AE, Atsumi S. 2016. Cyanobacterial chemical production. J Biotechnol 231:106–114. https://doi.org/10.1016/j.jbiotec.2016.05.023.
3. Anfelt J, Kaczmarzyk D, Shabestary K, Renberg B, Rockberg J, Nielsen J, Uhlén M, Hudson EP. 2015. Genetic and nutrient modulation of acetyl-CoA levels in Synechocystis for n-butanol production. Microb Cell Fact 14:167. https://doi.org/10.1186/s12934-015-0355-9.
4. Lee SY, Choi JH, Xu Z. 2003. Microbial cell-surface display. Trends Biotechnol 21:45–52. https://doi.org/10.1016/S0167-7799(02)00006-9.
5. Johns NI, Blazejewski T, Gomes AL, Wang HH. 2016. Principles for designing synthetic microbial communities. Curr Opin Microbiol 31:146–153. https://doi.org/10.1016/j.mib.2016.03.010.
6. Smith MJ, Francis MB. 2016. A designed A. vinelandii-S. elongatus coculture for chemical photoproduction from air, water, phosphate, and trace metals. ACS Synth Biol 5:955–961. https://doi.org/10.1021/acssynbio.6b00107.
7. Weiss TL, Young EJ, Ducat DC. 2017. A synthetic, light-driven consortium of cyanobacteria and heterotrophic bacteria enables stable polyhydroxybutyrate production. Metab Eng 44:236–245. https://doi.org/10.1016/j.ymben.2017.10.009.
8. Li T, Li CT, Butler K, Hays SG, Guarnieri MT, Oyler GA, Betenbaugh MJ. 2017. Mimicking lichens: incorporation of yeast strains together with sucrose-secreting cyanobacteria improves survival, growth, ROS removal, and lipid production in a stable mutualistic co-culture production platform. Biotechnol Biofuels 10:55. https://doi.org/10.1186/s13068-017-0736-x.
9. Vandamme D, Foubert I, Muylaert K. 2013. Flocculation as a low-cost method for harvesting microalgae for bulk biomass production. Trends Biotechnol 31:233–239. https://doi.org/10.1016/j.tibtech.2012.12.005.
10. Veiga E, De Lorenzo V, Fernández LA. 2003. Autotransporters as scaffolds for novel bacterial adhesins: surface properties of Escherichia coli cells displaying Jun/Fos dimerization domains. J Bacteriol 185:5585–5590. https://doi.org/10.1128/JB.185.18.5585-5590.2003.
11. Hoiczyk E, Hansel A. 2000. Cyanobacterial cell walls: news from an unusual prokaryotic envelope. J Bacteriol 182:1191–1199. https://doi.org/10.1128/JB.182.5.1191-1199.2000.
12. Liberton M, Berg RH, Heuser J, Roth R, Pakrasi HB. 2006. Ultrastructure of the membrane systems in the unicellular cyanobacterium Synechocystis sp. strain PCC 6803. Protoplasma 227:129–138. https://doi.org/10.1007/s00709-006-0145-7.
13. Šmarda J, Šmajs D, Komrska J, Krzyžánek V. 2002. S-layers on cell walls of cyanobacteria. Micron 33:257–277. https://doi.org/10.1016/S0968-4328(01)00031-2.
14. De Philippis R, Vincenzini M. 1998. Exocellular polysaccharides from cyanobacteria and their possible applications. FEMS Microbiol Rev 22:151–175. https://doi.org/10.1111/j.1574-6976.1998.tb00365.x.
15. Chungjatupornchai W, Fa-Aroonsawat S. 2008. Biodegradation of organophosphate pesticide using recombinant cyanobacteria with surface- and intracellular-expressed organophosphorus hydrolase. J Microbiol Biotechnol 18:946–951.
16. Chungjatupornchai W, Kamlangdee A, Fa-Aroonsawat S. 2011. Display of organophosphorus hydrolase on the cyanobacterial cell surface using Synechococcus outer membrane protein A as an anchoring motif. Appl Biochem Biotechnol 164:1048–1057. https://doi.org/10.1007/s12010-011-9193-3.
17. Fedeson DT, Ducat DC. 2017. Cyanobacterial surface display system mediates engineered interspecies and abiotic binding. ACS Synth Biol 6:367–374. https://doi.org/10.1021/acssynbio.6b00254.
18. Ferri S, Nakamura M, Ito A, Nakajima M, Abe K, Kojima K, Sode K. 2015. Efficient surface-display of autotransporter proteins in cyanobacteria. Algal Res 12:337–340. https://doi.org/10.1016/j.algal.2015.09.013.
19. Löfblom J, Feldwisch J, Tolmachev V, Carlsson J, Ståhl S, Frejd FY. 2010. Affibody molecules: engineered proteins for therapeutic, diagnostic and biotechnological applications. FEBS Lett 584:2670–2680. https://doi.org/10.1016/j.febslet.2010.04.014.
20. Nilsson B, Moks T, Jansson B, Abrahmsén L, Elmblad A, Holmgren E, Henrichson C, Jones TA, Uhlén M. 1987. A synthetic IgG-binding domain based on staphylococcal protein A. Protein Eng Des Sel 1:107–113. https://doi.org/10.1093/protein/1.2.107.
21. Trautner C, Vermaas WFJ. 2013. The sll1951 gene encodes the surface layer protein of Synechocystis sp. strain PCC 6803. J Bacteriol 195:5370–5380. https://doi.org/10.1128/JB.00615-13.
22. Bhaya D, Bianco NR, Bryant D, Grossman A. 2000. Type IV pilus biogenesis and motility in the cyanobacterium Synechocystis sp. PCC6803. Mol Microbiol 37:941–951. https://doi.org/10.1046/j.1365-2958.2000.02068.x.
23. Yoshihara S, Geng X, Okamoto S, Yura K, Murata T, Go M, Ohmori M, Ikeuchi M. 2001. Mutational analysis of genes involved in pilus structure, motility and transformation competency in the unicellular motile cyanobacterium Synechocystis sp. PCC 6803. Plant Cell Physiol 42:63–73. https://doi.org/10.1093/pcp/pce007.
24. Schuergers N, Wilde A. 2015. Appendages of the cyanobacterial cell. Life 5:700–715. https://doi.org/10.3390/life5010700.
25. Bhaya D, Watanabe N, Ogawa T, Grossman AR. 1999. The role of an alternative sigma factor in motility and pilus formation in the cyanobacterium Synechocystis sp. strain PCC6803. Proc Natl Acad Sci U S A 96:3188–3193.
26. Anfelt J, Hallström B, Nielsen J, Uhlén M, Hudson EP. 2013. Using

Downloaded from http://jb.asm.org/ on August 9, 2018 by TECH KNOWLEDGE CTR OF DENMARK

transcriptomics to improve butanol tolerance of Synechocystis sp. strain PCC 6803. Appl Environ Microbiol 79:7419–7427. https://doi.org/10.1128/AEM.02694-13.
27. Inaba M, Suzuki I, Szalontai B, Kanesaki Y, Los DA, Hayashi H, Murata N. 2003. Gene-engineered rigidification of membrane lipids enhances the cold inducibility of gene expression in Synechocystis. J Biol Chem 278:12191–12198. https://doi.org/10.1074/jbc.M212204200.
28. Wang H-L, Postier BL, Burnap RL. 2004. Alterations in global patterns of gene expression in Synechocystis sp. PCC 6803 in response to inorganic carbon limitation and the inactivation of ndhR, a LysR family regulator. J Biol Chem 279:5739–5751. https://doi.org/10.1074/jbc.M311336200.
29. Gunneriusson E, Nord K, Uhlén M, Nygren PÅ. 1999. Affinity maturation of a Taq DNA polymerase specific affibody by helix shuffling. Protein Eng 12:873–878. https://doi.org/10.1093/protein/12.10.873.
30. Mohamed A, Jansson C. 1989. Influence of light on accumulation of photosynthesis-specific transcripts in the cyanobacterium Synechocystis 6803. Plant Mol Biol 13:693–700. https://doi.org/10.1007/BF00016024.
31. Hospenthal MK, Costa TRD, Waksman G. 2017. A comprehensive guide to pilus biogenesis in Gram-negative bacteria. Nat Rev Microbiol 15:365–379. https://doi.org/10.1038/nrmicro.2017.40.
32. Oliveira P, Martins NM, Santos M, Pinto F, Büttel Z, Couto NAS, Wright PC, Tamagnini P. 2016. The versatile TolC-like Slr1270 in the cyanobacterium Synechocystis sp. PCC 6803. Environ Microbiol 18:486–502. https://doi.org/10.1111/1462-2920.13172.
33. Agarwal R, Whitelegge JP, Saini S, Shrivastav AP. 2018. The S-layer biogenesis system of Synechocystis 6803: role of Sll1180 and Sll1181 (E. coli HlyB and HlyD analogs) as type-I secretion components for Sll1951 export. Biochim Biophys Acta 1860:1436–1446. https://doi.org/10.1016/j.bbamem.2018.04.006.
34. Sakiyama T, Ueno H, Homma H, Numata O, Kuwabara T. 2006. Purification and characterization of a hemolysin-like protein, Sll1951, a nontoxic member of the RTX protein family from the cyanobacterium Synechocystis sp. strain PCC 6803. J Bacteriol 188:3535–3542. https://doi.org/10.1128/JB.188.10.3535-3542.2006.
35. Trautmann D, Voss B, Wilde A, Al-Babili S, Hess WR. 2012. Microevolution in cyanobacteria: re-sequencing a motile substrain of Synechocystis sp. PCC 6803. DNA Res 19:435–448. https://doi.org/10.1093/dnares/dss024.
36. Kanesaki Y, Shiwa Y, Tajima N, Suzuki M, Watanabe S, Sato N, Ikeuchi M, Yoshikawa H. 2012. Identification of substrain-specific mutations by massively parallel whole-genome resequencing of Synechocystis sp. PCC 6803. DNA Res 19:67–79. https://doi.org/10.1093/dnares/dsr042.
37. Nakao M, Okamoto S, Kohara M, Fujishiro T, Fujisawa T, Sato S, Tabata S, Kaneko T, Nakamura Y. 2010. CyanoBase: the cyanobacteria genome database update 2010. Nucleic Acids Res 38:D379–D381. https://doi.org/10.1093/nar/gkp915.
38. Kim YH, Park YM, Kim S-J, Park Y-I, Choi J-S, Chung Y-H. 2004. The role of Slr1443 in pilus biogenesis in Synechocystis sp. PCC 6803: involvement in post-translational modification of pilins. Biochem Biophys Res Commun 315:179–186. https://doi.org/10.1016/j.bbrc.2004.01.036.
39. Kim YH, Kim JY, Kim S-Y, Lee JH, Lee JS, Chung Y-H, Yoo JS, Park YM. 2009. Alteration in the glycan pattern of pilin in a nonmotile mutant of Synechocystis sp. PCC 6803. Proteomics 9:1075–1086. https://doi.org/10.1002/pmic.200800372.
40. Kim YH, Park KH, Kim S-Y, Ji ES, Kim JY, Lee SK, Yoo JS, Kim HS, Park YM. 2011. Identification of trimethylation at C-terminal lysine of pilin in the cyanobacterium Synechocystis PCC 6803. Biochem Biophys Res Commun 404:587–592. https://doi.org/10.1016/j.bbrc.2010.11.133.
41. Okamoto S, Ohmori M. 2002. The cyanobacterial PilT protein responsible for cell motility and transformation hydrolyzes ATP. Plant Cell Physiol 43:1127–1136. https://doi.org/10.1093/pcp/pcf128.
42. Gonzalez Rivera AK, Forest KT. 2017. Shearing and enrichment of extracellular type IV pili. Methods Mol Biol 1615:311–320. https://doi.org/10.1007/978-1-4939-7033-9_25.
43. Wernérus H, Ståhl S. 2002. Vector engineering to improve a staphylococcal surface display system. FEMS Microbiol Lett 212:47–54. https://doi.org/10.1111/j.1574-6968.2002.tb11243.x.
44. Andréoni C, Goetsch L, Libon C, Samuelson P, Nguyen TN, Robert A, Uhlén M, Binz H, Ståhl S. 1997. Flow cytometric quantification of surface-displayed recombinant receptors on staphylococci. Biotechniques 23:696–704.
45. Fleetwood F, Andersson KG, Ståhl S, Löfblom J. 2014. An engineered autotransporter-based surface expression vector enables efficient display of affibody molecules on OmpT-negative E. coli as well as protease-mediated secretion in OmpT-positive strains. Microb Cell Fact 13:179. https://doi.org/10.1186/s12934-014-0179-z.
46. Eklund M, Axelsson L, Uhlén M, Nygren P-Å. 2002. Anti-idiotypic protein domains selected from protein A-based affibody libraries. Proteins 48:454–462. https://doi.org/10.1002/prot.10169.
47. Lacey RF, Binder B. 2016. Ethylene regulates the physiology of the cyanobacterium Synechocystis sp. PCC 6803 via an ethylene receptor. Plant Physiol 171:2798–2809. https://doi.org/10.1104/pp.16.00602.
48. Nagar E, Zilberman S, Sendersky E, Simkovsky R, Shimoni E, Gershtein D, Herzberg M, Golden SS, Schwarz R. 2017. Type 4 pili are dispensable for biofilm development in the cyanobacterium Synechococcus elongatus. Environ Microbiol 19:2862–2872. https://doi.org/10.1111/1462-2920.13814.
49. Schindelin J, Arganda-Carreras I, Frise E, Kaynig V, Longair M, Pietzsch T, Preibisch S, Rueden C, Saalfeld S, Schmid B, Tinevez J-Y, White DJ, Hartenstein V, Eliceiri K, Tomancak P, Cardona A. 2012. Fiji: an open-source platform for biological-image analysis. Nat Methods 9:676–682. https://doi.org/10.1038/nmeth.2019.
50. Maeda Y, Tateishi T, Niwa Y, Muto M, Yoshino T, Kisailus D, Tanaka T. 2016. Peptide-mediated microalgae harvesting method for efficient biofuel production. Biotechnol Biofuels 9:10. https://doi.org/10.1186/s13068-015-0406-9.
51. Hudson EP, Uhlen M, Rockberg J. 2012. Multiplex epitope mapping using bacterial surface display reveals both linear and conformational epitopes. Sci Rep 2:706. https://doi.org/10.1038/srep00706.
52. Nilvebrant J, Hober S. 2013. The albumin-binding domain as a scaffold for protein engineering. Comput Struct Biotechnol J 6:e201303009. https://doi.org/10.5936/csbj.201303009.
53. Löfblom J, Wernérus H, Ståhl S. 2005. Fine affinity discrimination by normalized fluorescence activated cell sorting in staphylococcal surface display. FEMS Microbiol Lett 248:189–198. https://doi.org/10.1016/j.femsle.2005.05.040.
54. Andersson KG. 2017. Combinatorial protein engineering of affibody molecules using E. coli display and rational design of affibody-based tracers for medical imaging. PhD thesis. KTH Royal Institute of Technology, Stockholm, Sweden.
55. Schembri MA, Klemm P. 2000. Fimbrial surface display systems in bacteria: from vaccines to random libraries. Microbiology 146:3025–3032. https://doi.org/10.1099/00221287-146-12-3025.
56. Tippmann S, Anfelt J, David F, Rand JM, Siewers V, Uhlén M, Nielsen J, Hudson EP. 2017. Affibody scaffolds improve sesquiterpene production in Saccharomyces cerevisiae. ACS Synth Biol 6:19–28. https://doi.org/10.1021/acssynbio.6b00109.
57. Ducat DC, Avelar-Rivas JA, Way JC, Silver PA. 2012. Rerouting carbon flux to enhance photosynthetic productivity. Appl Environ Microbiol 78:2660–2668. https://doi.org/10.1128/AEM.07901-11.
58. Savakis P, Tan X, Du W, Branco Dos Santos F, Lu X, Hellingwerf KJ. 2015. Photosynthetic production of glycerol by a recombinant cyanobacterium. J Biotechnol 195:46–51. https://doi.org/10.1016/j.jbiotec.2014.12.015.
59. Zhang Z, Meng L, Ni C, Yao L, Zhang F, Jin Y, Mu X, Zhu S, Lu X, Liu S, Yu C, Wang C, Zheng P, Wu J, Kang L, Zhang HM, Ouyang Q. 2017. Engineering Escherichia coli to bind to cyanobacteria. J Biosci Bioeng 123:347–352. https://doi.org/10.1016/j.jbiosc.2016.09.010.
60. Uduman N, Qi Y, Danquah MK, Forde GM, Hoadley A. 2010. Dewatering of microalgal cultures: a major bottleneck to algae-based fuels. J Renew Sustain Energy 2:012701. https://doi.org/10.1063/1.3294480.
61. Care A, Bergquist PL, Sunna A. 2015. Solid-binding peptides: smart tools for nanobiotechnology. Trends Biotechnol 33:259–268. https://doi.org/10.1016/j.tibtech.2015.02.005.
62. Shiba K. 2010. Exploitation of peptide motif sequences and their use in nanobiotechnology. Curr Opin Biotechnol 21:412–425. https://doi.org/10.1016/j.copbio.2010.07.008.
63. Winther-Larsen HC, Wolfgang M, Dunham S, van Putten JPM, Dorward D, Løvold C, Aas FE, Koomey M. 2005. A conserved set of pilin-like molecules controls type IV pilus dynamics and organelle-associated functions in Neisseria gonorrhoeae. Mol Microbiol 56:903–917. https://doi.org/10.1111/j.1365-2958.2005.04591.x.
64. Carbonnelle E, Helaine S, Nassif X, Pelicic V. 2006. A systematic genetic analysis in Neisseria meningitidis defines the Pil proteins required for assembly, functionality, stabilization and export of type IV pili. Mol Microbiol 61:1510–1522. https://doi.org/10.1111/j.1365-2958.2006.05341.x.
65. Giltner CL, Habash M, Burrows LL. 2010. Pseudomonas aeruginosa minor pilins are incorporated into type IV pili. J Mol Biol 398:444–461. https://doi.org/10.1016/j.jmb.2010.03.028.

Downloaded from http://jb.asm.org/ on August 9, 2018 by TECH KNOWLEDGE CTR OF DENMARK

66. Nguyen Y, Sugiman-Marangos S, Harvey H, Bell SD, Charlton CL, Junop MS, Burrows LL. 2015. Pseudomonas aeruginosa minor pilins prime type IVa pilus assembly and promote surface display of the PilY1 adhesin. J Biol Chem 290:601–611. https://doi.org/10.1074/jbc.M114.616904.
67. Ng D, Harn T, Altindal T, Kolappan S, Marles JM, Lala R, Spielman I, Gao Y, Hauke CA, Kovacikova G, Verjee Z, Taylor RK, Biais N, Craig L. 2016. The Vibrio cholerae minor pilin TcpB initiates assembly and retraction of the toxin-coregulated pilus. PLoS Pathog 12:e1006109. https://doi.org/10.1371/journal.ppat.1006109.
68. Kamei A, Yuasa T, Orikawa K, Geng XX, Ikeuchi M. 2001. A eukaryotic-type protein kinase, SpkA, is required for normal motility of the unicellular cyanobacterium Synechocystis sp. strain PCC 6803. J Bacteriol 183:1505–1510. https://doi.org/10.1128/JB.183.5.1505-1510.2001.
69. Nakane D, Nishizaka T. 2017. Asymmetric distribution of type IV pili triggered by directional light in unicellular cyanobacteria. Proc Natl Acad Sci U S A 114:6593–6598. https://doi.org/10.1073/pnas.1702395114.
70. Bingle WH, Nomellini JF, Smit J. 1997. Linker mutagenesis of the Caulobacter crescentus S-layer protein: toward a definition of an N-terminal anchoring region and a C-terminal secretion signal and the potential for heterologous protein secretion. J Bacteriol 179:601–611. https://doi.org/10.1128/jb.179.3.601-611.1997.
71. Nomellini JF, Duncan G, Dorocicz IR, Smit J. 2007. S-layer-mediated display of the immunoglobulin G-binding domain of streptococcal protein G on the surface of Caulobacter crescentus: development of an immunoactive reagent. Appl Environ Microbiol 73:3245–3253. https://doi.org/10.1128/AEM.02900-06.
72. Huang HH, Camsund D, Lindblad P, Heidorn T. 2010. Design and characterization of molecular tools for a synthetic biology approach towards developing cyanobacterial biotechnology. Nucleic Acids Res 38:2577–2593. https://doi.org/10.1093/nar/gkq164.
73. Don RH, Cox PT, Wainwright BJ, Baker K, Mattick JS. 1991. 'Touchdown' PCR to circumvent spurious priming during gene amplification. Nucleic Acids Res 19:4008. https://doi.org/10.1093/nar/19.14.4008.
74. Engler C, Kandzia R, Marillonnet S. 2008. A one pot, one step, precision cloning method with high throughput capability. PLoS One 3:e3647. https://doi.org/10.1371/journal.pone.0003647.
75. Cheah YE, Albers SC, Peebles CAM. 2013. A novel counter-selection method for markerless genetic modification in Synechocystis sp. PCC 6803. Biotechnol Prog 29:23–30. https://doi.org/10.1002/btpr.1661.
76. Imam S, Chen Z, Roos DS, Pohlschröder M. 2011. Identification of surprisingly diverse type IV pili, across a broad range of Gram-positive bacteria. PLoS One 6:e28919. https://doi.org/10.1371/journal.pone.0028919.
77. Muñoz-Gutiérrez I, Moss-Acosta C, Trujillo-Martinez B, Gosset G, Martinez A. 2014. Ag43-mediated display of a thermostable β-glucosidase in Escherichia coli and its use for simultaneous saccharification and fermentation at high temperatures. Microb Cell Fact 13:106. https://doi.org/10.1186/s12934-014-0106-3.
78. Nakasugi K, Svenson CJ, Neilan BA. 2006. The competence gene, comF, from Synechocystis sp. strain PCC 6803 is involved in natural transformation, phototactic motility and piliation. Microbiology 152:3623–3631. https://doi.org/10.1099/mic.0.29189-0.
79. Walker SG, Smith SH, Smit J. 1992. Isolation and comparison of the paracrystalline surface layer proteins of freshwater caulobacters. J Bacteriol 174:1783–1792. https://doi.org/10.1128/jb.174.6.1783-1792.1992.

Downloaded from http://jb.asm.org/ on August 9, 2018 by TECH KNOWLEDGE CTR OF DENMARK